Forschungszentrum Karlsruhe
Technik und Umwelt

Wissenschaftliche Berichte
FZKA 6186
EXV-CSC(99)-D036

The COMET Concept for Cooling Core Melts: Evaluation of the Experimental Studies and Use in the EPR

H. Alsmeyer, W. Tromm

Institut für Kern- und Energietechnik
Projekt Nukleare Sicherheitsforschung

Oktober 1999

Forschungszentrum Karlsruhe

Technik und Umwelt

Wissenschaftliche Berichte

FZKA 6186

EXV-CSC(99)-D036

The COMET Concept for Cooling Core Melts: Evaluation of the Experimental Studies and Use in the EPR

H. Alsmeyer, W. Tromm

Institut für Kern- und Energietechnik
Projekt Nukleare Sicherheitsforschung

Forschungszentrum Karlsruhe GmbH, Karlsruhe
1999

Als Manuskript gedruckt

Forschungszentrum Karlsruhe GmbH
Postfach 3640, 76021 Karlsruhe

Mitglied der Hermann von Helmholtz-Gemeinschaft
Deutscher Forschungszentren (HGF)

ISSN 0947-8620

Preface

In Germany, future light water reactors are planned to be equipped with additional technical installations for the safe management of core meltdown accidents. To reach the objective of a safe enclosure of radioactivity in the reactor building, the COMET cooling concept is being developed. After melt-through of the reactor pressure vessel, the core melt shall be caught and cooled down safely.

The present report gives a survey of the previous extensive studies on the COMET cooling concept and its possible use in the EPR. The report shall serve as a decision aid as regards the use of COMET concept in the EPR and as a basis for discussions on possible further developments.

The following persons are involved in the experiments on the COMET concept:

H. Benz, C. Grehl, G. Merkel, W. Ratajczak, (HVT); W. Bohn, T. Cron, J.J. Foit, S. Schmidt-Stiefel, H. Schneider, T. Wenz (IKET); S. Mussa, F. Ferderer (KIKI); C. Adelhelm, M. Heinle (IMF 1); H.-G. Dillmann, H. Pasler (ITC-TAB); R. Buschbacher, W. Schöck (IMK); G. Schumacher (INR), M.T. Farmer, R.W. Aeschlimann, B.W. Spencer (ANL/USA)

This work is performed within the framework of the investigations for the development of the EPR by the Forschungszentrum Karlsruhe, Nuclear Safety Research Project in cooperation with and with the financial support of the German utilities and Siemens. The work is partially funded by the European Union under the 4^{th} and 5^{th} framework programs.

Abstract

The COMET concept of corium cooling is developed to arrest and cool ex-vessel corium melts in the case of core melt accidents. After erosion of a sacrificial concrete layer the melt is passively flooded by bottom injection of coolant water through a multitude of flow channels. The resulting evaporation process creates a porous structure of the melt from which the heat is easily extracted. Therefore, the porous melt solidifies within less than one hour typical and is permanently flooded by water.

The report describes various experiments which investigate the major processes during fragmentation and cooling of the melt. Very detailed experiments were performed with high-temperature thermite melts, in the form of transient tests or with decay heat simulation. These experiments were supplemented and confirmed by two experiments using UO_2-containing prototype corium melts. The dominant phenomena during cooling are described and it is shown that safe short-term and long-term cooling is achieved when a reasonable pressure of the flooding water exists. An advantage of the concept is the fast solidification of the melt which excludes chemical or thermal loads of the containment structure. The different aspects which are important for the application of the COMET cooling concept in the EPR are discussed to initiate further discussions and to facilitate the decision process with regard to the application.

A possible simplification of the concept is the replacement of the flooding channels by a porous, water-filled concrete layer, an option for which further investigations are planned.

Das COMET-Konzept zur Kühlung von Kernschmelzen:
Bewertung der experimentellen Untersuchungen und des Einsatzes im EPR

Zusammenfassung

Das COMET Konzept zur Kühlung von Kernschmelzen wird entwickelt, um Kernschmelzen, die im Falle eines schweren Reaktorunfalls entstehen können, außerhalb des Druckbehälters zu stoppen und zu kühlen. Nachdem die Schmelze eine Beton-Opferschicht erodiert hat, wird sie durch eine Vielzahl von Kühlkanälen von unten mit Wasser passiv geflutet. Durch den dadurch einsetzenden Verdampfungsvorgang ensteht eine poröse, durchströmte Schmelze, aus der die Wärme leicht abgeführt werden kann. Darum erstarrt die Schmelze innerhalb weniger als einer Stunde und bleibt vollständig mit Wasser geflutet.

Der Bericht beschreibt verschiedenartige Experimente, die die wichtigen Vorgänge während der Fragmentierung und Flutung untersuchen. Sehr detaillierte Untersuchungen wurden mit Thermitschmelzen durchgeführt, und zwar als transiente Experimente oder mit Simulation der Nachwärme. Diese Experimente werden ergänzt und bestätigt durch zwei Experimente mit prototypischen Kernschmelzen unter Einschluß von UO_2. Die wichtigsten Phänomene während der Kühlphase werden beschrieben und es wird gezeigt, daß eine sichere Kurz- und Langzeitkühlung der Schmelze erreicht wird, wenn das Flutwasser einen angemessenen Druck besitzt. Ein Vorteil des Kühlkonzepts ist die schnelle Erstarrung der Schmelze, die eine chemische oder thermische Belastung der Strukturen im Sicherheitsbehälter ausschließt. Die unterschiedlichen Aspekte, die für den Einsatz des COMET Kühlkonzepts im EPR von Bedeutung sind, werden besprochen, um weitere Diskussionen anzustossen und den Entscheidungsprozess bezüglich der Anwendung zu erleichtern.

Eine mögliche Vereinfachung des Konzepts ist der Ersatz der Kühlkanäle durch eine poröse, wasserführende Betonschicht. Für diese Variante sind weitere Untersuchungen geplant.

Contents

List of Figures

Page

List of Tables

1. Technical Description of the COMET Core Catcher

In the core catcher design (COMET concept) developed by the Forschungszentrum Karlsruhe, the core melt is converted into a porous, water-permeable layer for efficient cooling. The thus generated large internal surface area of the melt, which has a rather low thermal conductivity, allows an effective heat removal from the oxidic melt to the cooling water used for the passive flooding of the melt. The melt is subjected to fragmentation due to water penetration from below. The rapidly starting evaporation causes the melt to break up and solidify in a porous manner.

According to the design of the EPR containment, the core catcher device is located in the spreading compartment of the EPR (see Fig. 1.1). A previous proposal was to install the COMET cooling facility below the reactor pressure vessel [1]. This arrangement would have brought about advantages in terms of the spreading of the melt, its localization when released under pressure and the later drop of the residual melt.

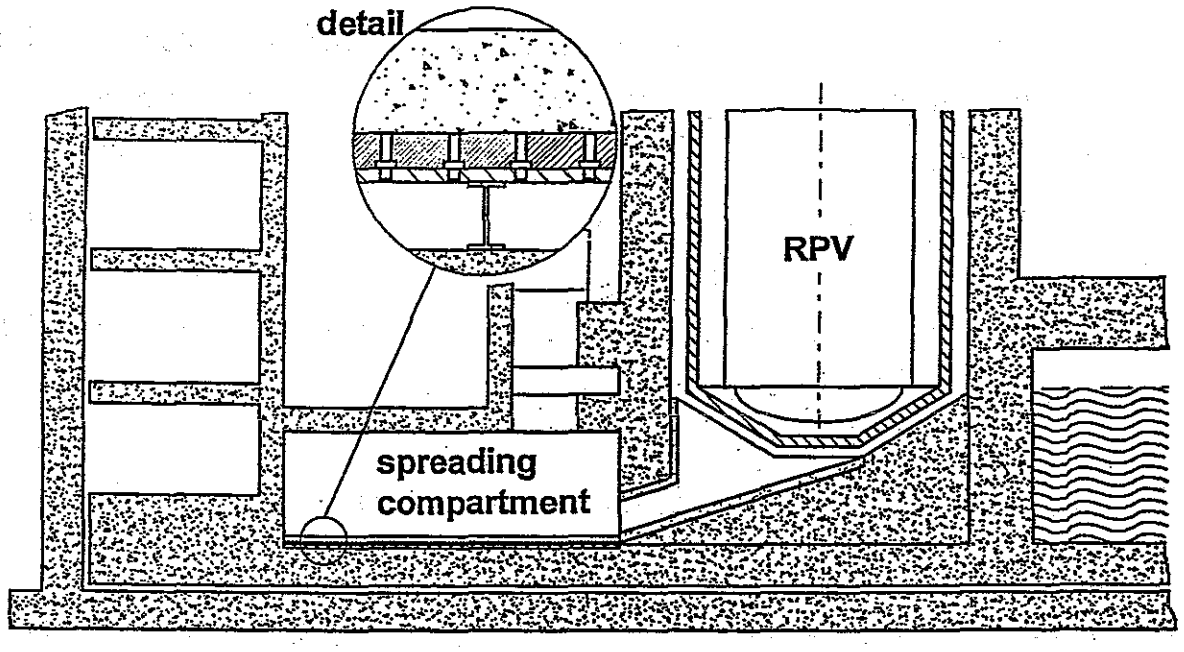

Fig. 1.1: **COMET concept with the cooling area arranged at the side of the RPV**

The cooling device consists of a perforated steel base plate that is coated by a ceramic Al_2O_3 grout layer and a sacrificial concrete layer on top. The sacrificial layer

has a height of about 15 cm. The Al_2O_3 layer contains cooling channels with melting caps that are arranged in line with the holes of the base plate. The base plate is fixed to the concrete foundation by double T-sections. The thus generated free gap is connected to the IRWST via a supply line. This IRWST is used for passive flooding during an accident situation. The core melt erodes the sacrificial layer until the Al_2O_3 layer is reached. The integrated melting caps are molten such that the water below can penetrate into the melt, break it up due to the rapid steam generation and leave the melt in upward direction. The melt is cooled down and starts to solidify before the Al_2O_3 protection layer is further eroded. Consequently, an attack on the base plate is avoided.

It is proposed to produce the sacrificial concrete layer from commercially available broken borosilicate glass, the composition of which corresponds to that of glasses applied for the vitrification of radioactive wastes. This sacrificial layer serves to promote the spreading of the melt by a reduction of the solidification temperature and a decrease in the viscosity of the melt. The melting of the sacrificial layer also causes the high initial temperature of the melt to drop below 2000°C. Furthermore, the materials in the sacrificial layer ensure oxidation of the possibly present metallic zirconium. Thus, major structures are prevented from being attacked chemically by the metallic zirconium. Moreover, a rapid Zr oxidation during subsequent water penetration and the resulting strong exothermic chemical reaction with a significant formation of hydrogen are avoided. Another major function of the sacrificial layer consists in the safe long-term binding of the fission products by the glass-forming components.

The major materials and components applied may be characterized as follows:

Sacrificial concrete of borosilicate glass in accordance with the composition used in the COMET-H experiments:

Aggregate material: Glass frit of borosilicate glass (manufacturer: Klaus Sorg company, Würzburg); main constituents 62.5 wt.% SiO_2, 14.5% Na_2O, 6% B_2O_3 of

the following grain sizes: 50% 0-1 mm, 15% 1-2 mm, 15% 2-4 mm, 20% 4-8 mm; amount required: 1603 kg/m^3 concrete.

Cement content: 415 kg/m^3 concrete; water content: 236 l/m^3 concrete; flux 12.45 l/m^3 concrete; bulk density 2267 kg/m^3 concrete.

The concrete can be processed and compressed easily.

Ceramic Al_2O_3 Grout Layer:

The material applied (manufacturer: ALCOA Chemie, Ludwigshafen, designation: Tabularoxid SFL 205) is employed for lining ladles in steel production. When applied, it has a very good flowability and spreads automatically due to its thixotropic behavior (low viscosity during spreading) without a compression being necessary. Its bulk density amounts to 3180 kg/m^3. The material is not subjected to a heat treatment for use in COMET (contrary to its use in steel industry).

The layer has a height of 50 mm and is just in line with the upper edge of the cooling channels.

Carrier Plate and Double T-sections:

Made of structural steel, designed against dynamic loads which may occur due to weak, steam explosion-like processes during the melt/water contact.

Cooling Channels (Melting Plugs):

Arrangement in a square grid of 80 x 80 mm, setup according to Fig. 1.2. Height from the steel plate up to the upper edge 50 mm. The melting plugs are produced from plastic (e.g. polycarbonate or polysulfone) by injection moulding. At the upper ends, they are equipped with burnable caps that are sealed against humidity. The diameter of the throttle that limits the water inflow into the melt is 5 mm. The melting plugs are inserted into the holes of the carrier plate from above (upon the assembly of the

carrier plate in the spreading compartment). They are self-locking by spring tongues located on the bottom side of the plate. Sealing against the water from below is ensured by an elastic rubber seal, e.g. in the bore of the plate.

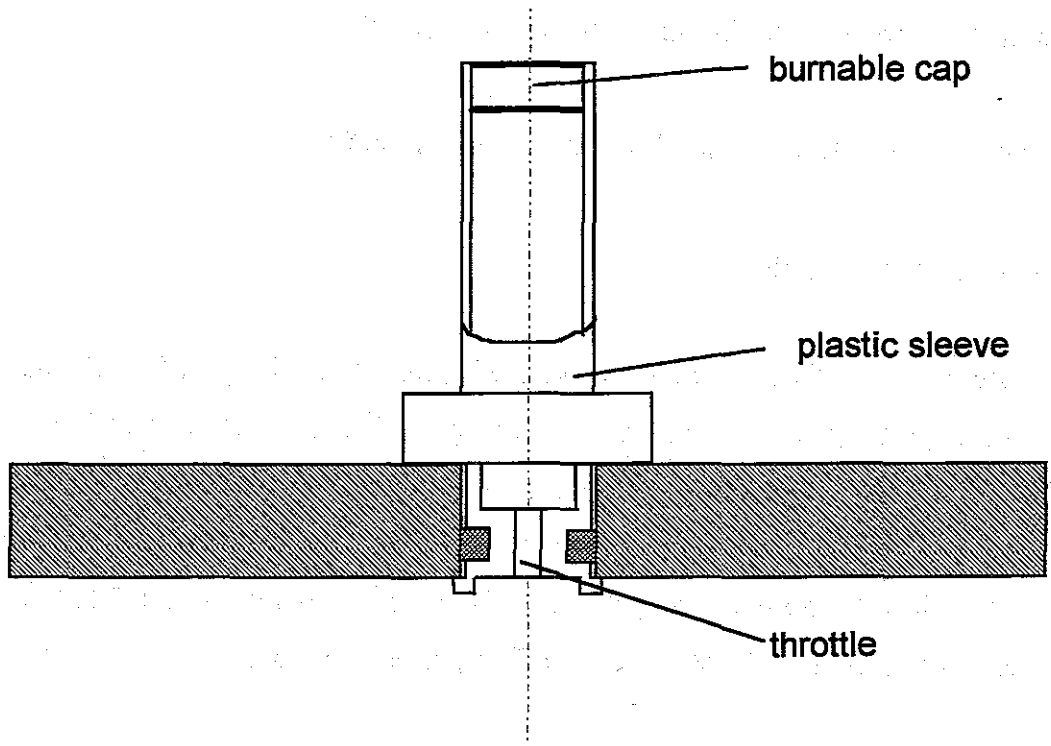

Fig. 1.2: **Melting plug with burnable cap for water inflow**

The burnable cap consists of a stoichiometric mixture of Mg powder and $KClO_4$ that is pressed to a pellet in a thin-walled aluminum cap. When inserting it into the plastic can, the pellet surface is coated with epoxide resin in order to prevent the penetration of humidity. This setup proved successful in all COMET experiments, especially because the effect of humidity is restricted to the phase of concrete setting and the cooling facility is dry afterwards.

The burnable cap ignites at a temperature of about 500°C. MgO and KCl are generated under high local heat release without major gas emissions such that the cap is molten completely and the cooling channel is unblocked.

Cooling Water Supply:

Cooling water is supplied from an above reservoir, e.g. from the IRWST. The effective cooling water pressure, i.e. the overpressure of the flooding water relative to the static pressure of the liquid melt with a height of about 37 cm, should be 0.2 bar or more.

The IRWST connection line is opened by a temperature-controlled valve which is triggered by high temperatures at the inlet of the spreading compartment. Alternatively, the melting of ropes stretched through the melt may cause the valves to open. When flooding the gap below the carrier plate, the air escapes via an ascending pipe. Functioning is not affected by the air remaining in the melting plugs.

2. Processes during Cooling

The major processes that ensure both short-term and long-term cooling of the core melt as envisaged by the COMET concept shall be explained in the following sections:

Spreading of the Melt

When leaving the reactor cavity, the melt flows onto the dry sacrificial concrete layer of the core catcher device and spreads. According to calculations made by Siemens, a melt height of about 37 cm is expected. For this spreading process sufficient time is available, because the intensive cooling of the melt by the flooding water only starts after the sacrificial concrete layer has been eroded by the melt. Depending on the initial state of the melt, this takes at least ten minutes. As obvious from the COMET-H experiments, the melt is agitated considerably not only by concrete erosion, but also by the initial flooding processes. Consequently, homogeneous spreading of the melt over the entire area can be assumed. This also means that in this time interval last runnings of residual melts are mixed and homogenized well with the base melt.

Erosion of the Sacrificial Concrete Layer

Due to the high temperature of the melt, erosion of the sacrificial concrete layer starts immediately. Erosion takes place under strong gas release according to the water fraction contained in the concrete. As a consequence, the temperatures and the compositions in the layers of the melt are homogenized. The following conclusions were drawn from previous investigations of the melt/concrete interaction:

- The erosion rate of the concrete is mainly determined by the composition of the melt. The highest erosion rate is reached when the overheated metal fraction is located below and not yet oxidized Zr metal exists. Under these conditions, a 15 cm high concrete layer was eroded after 10 minutes in the COMET-H-3.1

experiment. Then, water penetration takes place. In all other cases, the erosion rate is smaller, e.g. in the absence of metallic Zr due to its prior oxidation or in case of mixed metal and oxide melts, the heat transfer behavior of which largely corresponds to that of oxide melts.

- The molten concrete constituents completely mix with the oxide melt and cause its temperature and material parameters to change. Due to the low-melting components in the sacrificial concrete, the solidification temperature (liquidus/solidus interval) of the diluted oxide melt is decreased. Furthermore these components also reduce the viscosity, which is a rather favorable effect. A considerable decrease in the temperature of the melt is expected to cause a partial crystallization of the high-melting components ($UO_2 + ZrO_2$) in the oxide melt. These crystals increase the viscosity of the strongly agitated melt and, as a consequence, heat transfer to the concrete is reduced. This is a self-stabilizing process, by means of which the viscosities of the oxide melt during concrete erosion will be set to 0.1 - 10 Pa s at a temperature below 2000°C. These statements will possibly have to be verified when the temperatures of the melt leaving the reactor cavity will have been determined more reliably and the solidification ranges of corium melts with the composition expected will be better known.

- Due to the incorporation of the concrete, the density of the oxide melt is further reduced. It then becomes lighter than the metal melt. But it is not yet clear in our opinion, whether the metal melt will actually deposit at the bottom. Depending on the gas release, the incorporation of the metal into the oxide may be very intensive during the phase of nearly identical densities and, thus, cause small metal particles to be generated that deposit rather slowly or incompletely. It is therefore very important that cooling by water penetration from below takes place independently of the initial stratification of the melt.

- The major chemical reactions during concrete erosion are (1) the complete oxidation of the residual zirconium and (2) the release of hydrogen by the reduction of the steam in contact with metal in the order of Zr, Cr and Fe.

Process (1) is desired as the chemical aggressiveness of the melt is reduced considerably by the burn-out of Zr. In contrast to this, process (2) cannot be avoided and will have to be managed as far as the maximum hydrogen concentrations in the containment are concerned. It may be eased within certain limits by a lower water content in the concrete. In general, the upper limit of hydrogen release is determined by the water fraction contained in the sacrificial concrete layer, which is reduced to H_2. In the cooling phase following water inflow, only a small amount of hydrogen is produced.

- During concrete erosion aerosols are formed, which are released from the melt together with the gases. According to the COMET-H experiments, the aerosols mainly consist of the oxides of K and Na (K_2O and Na_2O), whereas less volatile fission products that still exist in the melt during this phase were hardly released. Aerosol formation strongly depends on the temperature and the chemical composition of the melt. According to the COMET experiments, it practically drops to zero as soon as cooling starts by water penetration from below.

Start of Cooling

As soon as the cooling channels are opened, the water enters the melt from below. At first, the inflowing water is evaporated immediately and completely due to the high temperature of the melt. The steam passes through the melt and breaks it up. This process is controlled above all by the volume increase during evaporation. By water evaporation at 100°C, the volume is increased by a factor of 1600. Further heating of the steam to about 1000 K, as expected when leaving the melt, causes the steam volume to increase again by a factor of 2.7. The typical inflow rate of an open cooling channel is 30 ml/s. This yields 50 l/s saturated steam or 130 l/s superheated steam. The high efficiency of fragmentation can be explained by this high volume increase inside the melt.

As long as the melt is in the liquid state, the generated flow channels are not stable, but constantly redeveloped in the turbulent melt. The direct water contact and the evaporation lead to a rapid cooling of the melt which then starts to solidify.

Solidification preferably starts in the vicinity of the flow inlets. As a result, erosion of the sacrificial concrete and loading of the ceramic base layer stop. Solidification proceeds from the bottom to the top. In the course of this process, the flow channels, through which the steam/water mixture escapes, stabilize. As the solidification of the oxide phase takes place by the formation of a highly viscous melt over a large temperature interval, the porous structure in the oxide melt is better developed than in the metal melt which remains rather thin-bodied until solidification and solidifies over a very narrow temperature range only. Finally, a solidified melt of high open porosity is obtained, which is passed by the water/steam mixture and flooded. Decay heat removal takes place by stationary boiling processes of the solidified melt at a low temperature.

As far as the necessary fragmentation of the melt is concerned, the question arises as to which maximum size non-fragmented, i.e. compact sections of the melt may be tolerated to ensure the desired complete solidification by water contact at the surface, and in spite of the production of decay heat inside the melt. The most unfavorable case is plane geometry. A plane layer of the thickness d, the surfaces of which are both in contact with water, solidifies completely, when

$$d \leq 2 \cdot \sqrt{\Delta T \cdot 2\lambda / q}$$

applies. Here, d denotes the thickness of the compact section, λ is its thermal conductivity, q the decay heat power density and ΔT the permissible temperature difference between the center and the cooled periphery.

For an oxidic melt these values are estimated pessimistically as follows: $\Delta T = 1300$ K, $\lambda = 1$ W/m·K, $q = 0.8$ MW/m^3. Here, the release of decay heat corresponds to the value obtained two hours after shutdown. The reduction of the decay heat density in the oxide by the dilution with molten concrete is neglected. This yields a permissible thickness of 11.4 cm.

For a steel melt the values of $\Delta T = 1300$ K, $\lambda = 30$ W/m·K and $q = 0.3$ MW/m^3 result in a permissible thickness of 100 cm. The much larger coolable layer thickness of

steel is mainly due to the higher conductivity and the lower decay heat power density which is smaller by a factor of 3. This means that cooling of steel melt usually does not cause any problems.

The thus estimated permissible dimensions of non-fragmented sections indicate the extent of fragmentation required and to be achieved by the formation of porous structure. However, inflow and contact with water must be sufficient to ensure continuous water and steam flow through the porous solidified melt. This is also promoted by the inflowing cooling water and the leaving steam having the same flow direction (no counterflow of water and steam).

Long-term Cooling

As a result of the complete solidification of the melt, which is expected to take about 30 minutes according to the COMET-H-experiments, thermal energy is largely removed from the melt. The solidified and flooded melt consequently has a low temperature of somewhat above 100°C over the long term. This means that the structures of the cooling facility and their surroundings have a permanently low temperature as they are in contact with the flooding water. This was also demonstrated in the COMET-H-experiments with a simulated decay heat generation. For the long-term removal of the decay heat, an integral cooling water supply of 10 l water/s is sufficient to compensate for the evaporation losses.

Further Aspects

The following processes have to be considered for a safe operation of the cooling facility:

- When the cooling channels are opened, the melt may penetrate through the plugs into the water layer below under certain conditions. This process depends on the cross-section of the plugs, the water pressure and the height and state of the melt.

- Direct contact between the melt and the cooling water may in principle result in steam explosions. It was shown by the numerous COMET experiments performed so far, however, that no sudden reactions with a significant pressure rise due to the injection of water occur during flooding from below. This also applies to experiments with UO_2-containing melts. It was demonstrated by the COMET-T experiments, where steam explosions were triggered off by extreme experimental conditions and the mechanical loads were quantified, that the reacting amounts of water are so small due to their pointed supply via the cooling channels that there is no danger of a steam explosion. As obvious from the COMET experiments, steam explosions can be excluded for the contact mode of water on melt during flooding from below because the melts have already cooled down considerably. Only in case of a massive supply of water directly onto the surface of the still very hot melt, which may possibly be initiated by certain processes in the primary circuit, sudden reactions may take place.

- Due to the size of the cooling area in the EPR, it may be assumed that the cooling channels do not open simultaneously, but start to open at certain sections first. This gives rise to the question, whether the cooling facility is sufficiently stable to stop downward erosion and whether flooding of a part of the melt adversely affects the coolability of other parts. This was studied experimentally and led to the use of the ceramic base layer which embeds the cooling channels and is supposed to be stable for a time that is sufficient for the solidification of the melt in the vicinity of the plugs. With this improvement, safe cooling was achieved in any case at an effective flooding water pressure of 0.2 bar. Even the onset of flooding and solidification of the melt surface in regions that were not yet passed by the cooling water did not adversely affect the coolability.

- Under extreme situations, impurities of the circulating flooding water by major dirt particles during long-term operation might block the flow paths. This can be avoided by water filtration upstream of the suction line of the pump and seems to be very reasonable with regard to the operation of pump and heat exchanger. However, COMET-H experiments with continued heating even after complete solidification showed that an interruption of the cooling water flow from below has

no negative effects on safe cooling, since the water penetration from above is sufficient due to the high porosity of the solidified melt.

Objectives of the COMET Experiments Performed

The processes mentioned above were identified in the experiments and additional observations were recorded. The experiments and their major results shall be presented below. The following objectives are pursued:

- Experiments with transparent model melts in the laboratory scale serve to understand and describe the phenomenology of the processes taking place during the solidification of the melts by water penetration from below.

- In transient experiments using 50 to 100 kg high-temperature melts and sometimes real melts with a high UO_2/ZrO_2 fraction, the initial fragmentation and cooling processes in the melt are studied. Due to the flexibility of such experiments, special aspects such as steam explosions and later runnings of melts can be investigated.

- Finally, experiments with the simulation of decay heat serve to study the short- and long-term processes during the cooling of up to more than 1000 kg melt in a large 1:1 model section of the cooling device.

In these experiments the following aspects with respect to save cooling or critical conditions are dealt with:

- Sufficient heat removal from the melt
- Rapid solidification of the melt
- Influence of water pressure, plug arrangement and plug geometry on coolability
- Possible penetration of melt through the cooling channels/melting plugs
- Coolable layer heights of the melt
- Influence of the melt composition
- Chemical processes in the melt

- Characterization of the exhaust gases
- Release of aerosols and simulated fission products
- Heating of the core catcher structures
- Influence of inhomogeneous concrete erosion
- Consequences of possible steam explosions
- Coolability of late runnings of the melt

Section 4.4 discusses the results with respect to the application as obtained by the different experiments.

3. Phenomenological Studies of Porous Solidification

3.1 Experiments with Liquids of High Viscosity and Gas Inflow from Below

In the COMET core catcher concept, evaporation processes start as soon as water inflow into the hot melt begins [2], [3]. These evaporation processes cause the water/steam volume to increase considerably and eventually lead to the fragmentation and porous solidification of the melt. Pure hydrodynamic (isothermal) experiments were performed to find out whether fragmentation in viscous melts can be achieved by the injection of high gas flows alone or whether evaporation and solidification processes are necessary for the generation of a porous structure.

The test setup consists of a rectangular glass container with a transparent oil [4]. Air is blown in from below via an individual hole. Three silicone oils of varying viscosity are applied, M10 (η=0.01 Pa s), M100 (η=0.1 Pa s) and M1000 (η=1.0 Pa s). This covers a wide viscosity range which is representative of real core melts. The experiments performed at room temperature serve to investigate the bubble formation and possible channel generation at high gas inflow.

It is evident from the results obtained by these experiments that the formation of bubble swarms by the coalescence of ascending bubbles does not indicate any strong lateral mixing of the gas phase into the liquid, as the separated bubble swarms hardly propagate laterally into the liquid. Even in case of formation of a gas jet at very high gas flows there are no indications of a possibly stronger lateral mixing of the gas phase and the liquid, as branchings of the gas jet into the lateral parts of the liquid are not observed. This indicates that phenomena reported below are correlated to the processes of evaporation in the liquid and eventual solidification.

3.2 Experiments with Solidifying Metal and Plastic Melts

To investigate the coupling of thermodynamic and fluid dynamic processes during the fragmentation of melts by water inflow from below, experiments with hot metal melts and plastic melts were performed. Here, the transparent plastic melt applied

represented the oxidic fraction of the core melt with its amorphous solidification behavior. The viscosity range of these melts may be compared with that of silicate-rich melts in a core meltdown accident, as it is expected upon the erosion of the sacrificial concrete layer. A solder with physical properties similar to that of the metal fraction of the core melt is used as the metal melt. However, the temperatures in these experiments of about 200°C are significantly smaller than those during a core meltdown accident. Nevertheless, they allow to study the evaporation of the inflowing water. Hence, all phase changes, the solidification of the melt as well as the evaporation of the inflowing water, are simulated qualitatively in the experiments.

The test rig consists of a melt tank with a rectangular base area of 106 mm x 40 mm and a height of 200 mm. Via a single hole of 10 mm ∅, the flooding water is supplied to the melt tank at a preselected water pressure. The pressure of the water relative to the height of the melt bath is adjusted such that a water pressure of 0 bar means equal pressures of the melt and the water at the inflow hole.

It is shown by the experiments that fragmentation of the melt is based on the coupling of water inflow and subsequent water evaporation. The melt is broken up by the evaporation processes and solidifies in a porous manner. In experiments with pure plastic melts and plastic melts with dispersed liquid metal, for high to moderate flooding water pressures and high melt viscosity an individual flow channel develops first. The subsequent formation of branched channels is attributed to the generation of steam bubbles during the evaporation of the water that has entered the melt. Behind these steam bubbles, small channels filled with water develop and a funnel-shaped fragmentation cone, with it centre at the water entrance, is generated slowly. In case of direct contact of water with the metal melt, the high temperature conductivity of the metal causes a sudden steam formation and more vigorous reactions occur. Therefore, metal and plastic melts are mixed strongly and partially ejected from the tank.

All melts applied in these phenomenological experiments solidify in a fragmented state with the degree of fragmentation varying considerably. Melts of low viscosity and high thermal conductivity show a stronger interaction with the coolant water and

hence more fragmentation than melts of high viscosity and small thermal conductivity. This is the expected behavior as viscosity reduces the motion of the melt, while a higher conductivity leads to faster evaporation of the coolant water and hence to higher steam fluxes which foster the fragmentation. The experiments with higher thermite melts, however, as reported later, show that the fragmentation process of metals is reduced when the metal layer is covered by a viscous oxide layer which dampens the metal agitation. The flooding water pressure has a decisive influence on the fragmentation pattern and hence on the pressure loss of the water flow following solidification of the melt. At a high flooding water pressure, relatively wide channels of small flow resistance form in the melt. At a small flooding water pressure, the melt is also fragmented, but the pressure loss in the smaller channels formed in the melt is higher.

3.3 Conclusions from the Laboratory Experiments

The formation of bubble swarms by bubble disintegration is not considered an important mechanism that leads to a homogeneous fragmentation of the melts, as the bubble swarms generated do not propagate laterally into the liquid. Even in the case of gas jets, there are no indications as to the formation of multiple branchings of the gas channels, which are observed in hot melts.

In contrast to this, experiments with hot plastic and metal melts and the injection of water from below via an individual channel always exhibit an extensive mixing of the melt and the cooling medium with subsequent porous solidification.

Obviously, rapid evaporation of the water inside the hot melt, accompanied by the starting solidification of the melt and the resulting stabilization of flow channels is of major importance for the fragmentation processes.

4. Experimental Investigations Regarding the Functionality of the Concept

4.1 Transient Experiments with High-temperature Thermite Melts, COMET-T

Introduction

This test series with iron and oxide melts of high temperature is characterized by experimental conditions that are close to reality. The melts (without simulation of the decay heat) are applied at about 2150 K, erode a thin sacrificial layer and are flooded passively when the melting plugs are opened [4]. The major physical properties of the used thermite melts nearly correspond to those of the core melts in a core meltdown accident.

The temperatures in the experiment correspond to the calculated temperatures of the core melt after the erosion of the sacrificial concrete layer and, hence, at the beginning of cooling water inflow. For the corresponding situation in a reactor, two cases are distinguished: After erosion of the sacrificial layer, either a layer of the lighter oxide melt is located above the metal melt, or the metal melt is dispersed into the oxide melt due to the strong agitation of the melt by gas release. Both cases are realized in the experiments.

The test setup, see Fig. 4.1.1, is selected such that it corresponds to the real geometrical conditions in the vicinity of the cooling water inflow holes. Transferability of the results to the core catcher configuration is ensured by the use of:

- Melts of high temperature with similar physical properties
- Realistic melt pool heights
- The same heat flows and comparable energy contents of the melt
- The same sacrificial layer material
- The same melting plugs
- A variation of the flooding water pressure within the limits of the concept design

Test Setup

The physical processes to be investigated above all include the melt/concrete interaction and the subsequent fragmentation and cooling by the steam and water flow through the melt. The test setup (Fig. 4.1.1) consists of a horizontal surface area of 250 mm ∅ with a sacrificial concrete layer, into which the melting plugs for water supply are cast and onto which the hot melt is poured or generated. The melt is contained in a cylindrical steel tank with a ceramic lining. The test vessel is screwed to three load cells via three bolts to measure the weight of melt and coolant throughout the test. The load cells are supported by a horizontal steel plate.

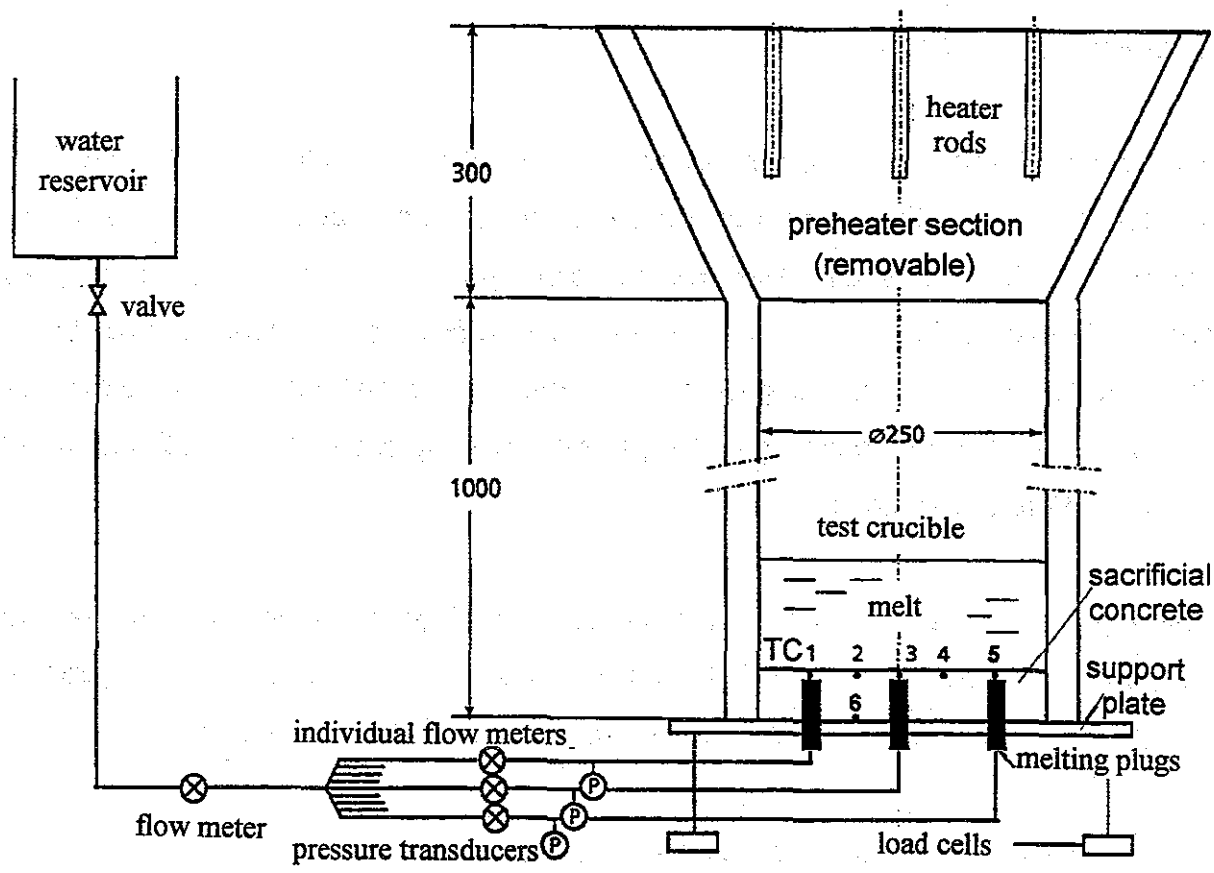

Fig. 4.1.1: **Setup used for experiments with high-temperature melts**

At first, the melting plugs obstruct water inflow. When the melt reaches the upper side of the plugs, they are molten and water inflow sets in. Via individual supply lines, the melting plugs are connected to a water distributing line which is connected to a water storage tank. This storage tank is supplied with water such that the water

level is always constant. By the geodetic height of the storage tank, the flooding water pressure can be set for each experiment. A flooding water pressure of 0 bar means that the geodetic height of the water column in the water storage tank just compensates the hydrostatic pressure of the melt at the upper edge of the melting plugs.

For the first test series, the melting plugs, including its tip, were made of the thermoplastic material of polyethylene. It was found, however, that the opening of these melting plugs was not satisfactory and had to be improved in terms of a sufficient water inflow. For this reason, a special melting plug was developed and tested. As mentioned in Sec. 1, page 4, this plug was equipped with a burnable cap. As a result, the melting plug opens so quickly that it cannot be stopped by the starting water flow. The thus improved melting plug proved efficient in the later experiments since it opened completely. Hence, it was applied for all further experiments, including the COMET-H tests.

Depending on the experiment, total height of the concrete layer on the base plate varied between 45 and 50 mm. It covered the melting plugs by 5 to 10 mm. Due to the absence of decay heat, the small coverage was chosen such as to facilitate the investigation of the water inflow phenomena.

The grain size distribution of the concrete aggregate in this test series is selected such that the concrete layer above the melting plugs is homogeneous in spite of the small coverage. The density of the sacrificial concrete is 2.2×10^3 kg/m^3. The chemical composition of the applied aggregate corresponds to that of the borosilicate glass proposed for the COMET concept.

For the simulation of the core melt, a melt of iron and aluminum oxide is applied. It is generated by means of a thermite reaction. A CaO fraction of 35 wt% is added to the thermite powder in order to influence the physical properties of the oxide portion of the melt. Thus, the solidification temperature of the oxide is reduced from that of pure Al_2O_3 (2323 K) to about 1670 K and the viscosity of the melt is decreased. This yields about 37 wt% of iron melt that is covered by a layer of 63 wt% oxide melt

(56% Al_2O_3 + 44% CaO). The initial temperature of the melt amounts to about 2150 K. The viscosity of the oxide melt generated is comparable with that of a corium melt upon the admixture of the sacrificial concrete.

The volume flows and pressures of the inflowing cooling water as well as the temperatures in the melting plugs, in the concrete layer and outside of the test vessel are measured. The load cells below the test vessel serve to measure the weight changes of the crucible. Together with the pressure measurements, they allow quantitative statements to be made with regard to possible vigorous melt/water interactions under water inflow. The test is monitored from above and from the side by means of video cameras.

In the test series, the effective flooding water pressure is varied between 0.0 and 0.4 bar. The melt mass applied ranges between 50 and 100 kg. In addition, 5 or 10 kg of Zr are added in some experiments. As another parameter, the height of the sacrificial layer above the melting plugs is reduced from the standard value of 10 mm to 5 mm. A survey of the major experiments is given in Table 4.1.1.

Table 4.1.1: Survey of the major transient COMET-T experiments

Experiment COMET-T	2.1	2.2	2.3	7.1	7.5	7.2	7.4	8.2	8.4	8.5	8.6
Melt mass, kg	54	54	54	54	54	59 +5 kg Zr	118 +10 kg Zr	65	72	56	64
Height of sacrificial layer above plugs, mm	5	5	5	10	10	10	10	10	10	10	10
Flooding water pressure, bar	0.2	0.0	0.4	0.2	0.0	0.2	0.2	0.2	0.4	0.0	0.2
Erosion time, min	0:20	0:51	0:33	2:26	3:00	2:13	1:42	4:50	1:30	1:25	1:20
Surface solidified, min	1:00	2:58	1:05	3:17	5:39	3:00	2:30	5:50	2:00	2:00	1:50
Surface covered with water, min	3:29	--	1:05	4:40	6:59	3:28	3:00	6:10	2:30	>2:30	2:34
Total water inflow rate, ml/s	171	101	210	185	135	310	400	100	425	180	330
Mean evaporation rate of water, l/s	--	--	--	100	65	150	200	50	150	70	120
Porosity in oxide/ metal, %	88/38	65/40	73/40	69/33	66/33	67/49	--/54	/30	/51	/30	/50

Test Results

The transient experiments shall be discussed under the following aspects: Fragmentation of the melt, and heat removal from the melt to the inflowing cooling water. Also, experiments with pure oxide melts shall be presented. Special experiments performed for studying the occurrence of steam explosions shall also be described.

Fragmentation

In principle, it was demonstrated by the experiments that melts of high temperature can be cooled very rapidly by water inflow from below. This is mainly due to the high porosity generated in the melt. Rapid evaporation of the inflowing cooling water is understood to be the dominating fragmentation mechanism. The bubbles produced by the evaporation expand in the melt. This leads to instabilities of the bubbles, and bubbles disintegrate due to their high ascending velocity. On the other hand, turbulent agitation of the bath also contributes to bubble disintegration. Consequently, a high gas volume fraction is generated in the melt, which causes extensive fragmentation. During solidification, cooling water penetrates into these cavities and provides for the long-term cooling of the melt.

Porosity of the solidified melt amounts to about 50% in the oxide and, hence, exceeds that of the metal (about 30%) which is layered below the oxide. Porosity is calculated from the ratio of the void to the volume of the solidified porous layer. The differences between the metal and the oxide melt in the layered situation are attributed to the viscosity behavior as a function of temperature. The liquid metal has a constant and low viscosity as compared to the oxide. It solidifies with a rapid phase change when cooled. In contrast to this, viscosity in the oxide strongly increases with decreasing temperature. Consequently, the rise time of gas bubbles in the oxide is considerably higher than in the metal layer when the melt starts to solidify, resulting in a higher porosity in the solid state. The higher void and residence time of gas bubbles was also observed in the experiments with gas injection into silicone oils.

It is evident from the crucible sections that very large, open cavities develop in the solidified oxide melt. In the solidified metal layer above the melting plugs, free connected flow channels are visible, see Fig. 4.1.2. The experiments show that metal and oxide melts can be cooled reliably up to an initial height of 50 cm. The layer height of the metal amounts to about 10 cm, that of the oxide to about 40 cm.

Fig. 4.1.2: **Section of the porous solidified metal layer**

Solidification time of the melt primarily depends on the pressure of the cooling water. In the experiments performed at a flooding water pressure of 0.2 and 0.4 bar, the melt solidifies within about 1 minute upon the start of water inflow, whereas generally longer solidification times are observed in the experiments at 0 bar flooding water pressure. In addition, the porosity of the solidified melt is smaller in the experiments at 0 bar flooding water pressure, which also causes the water inflow rate to be small.

When water inflow starts, the entire inflowing cooling water evaporates over a period of 30-50 s. Depending on the water inflow conditions, the heat flow removed to the entering cooling water in these transient tests is about 0.5 MW. Related to the base area of the cooling facility, this value exceeds that of the heat flow to be removed stationarily from the core melt due to decay heat generation by more than one order of magnitude.

Test Series with Pure Oxide Melts

In this test series the coolability of melts consisting of an oxide fraction only is investigated. As far as the composition of the melt is concerned, this case is considered a boundary case with the metal fraction in the core melt being small or mixed into the oxide melt in the form of small drops during concrete erosion. The behavior of a thus dispersed two-component melt corresponds to that of a pure oxide melt, as the oxide melt is the continuous phase and predominates in terms of the volume fraction.

The principle test setup is maintained. The thermite melt with the CaO additive, however, is no longer generated directly in the test vessel, but ignited in a separate thermite reaction crucible. After about 1 minute, the metal part o the melt is discharged into a container and the oxidic fraction of the melt is passed to the test vessel via the spout. To allow comparison with two-component thermite melts, the same test parameters are set.

Also the oxide experiments clearly demonstrate the dependence of the solidification behavior on water pressure. At a high water pressure of 0.4 bar in experiment 8.4, the melt is whirled up considerably by the first water contact and solidifies with a high porosity of 60%. This results in a high water inflow rate of 425 ml/s. The two experiments performed at a water pressure of 0.2 bar exhibit a very similar behavior. The water flows are larger than 250 ml/s and the porosity is higher than 50%.

At a water pressure of 0 bar in experiment 8.5, the interaction of the melt with the inflowing water is weaker, no melt is thrown out of the test vessel and the porosity of the solidified melt is smaller (about 30%). The maximum volume flow rate amounts to 180 ml/s and, hence, is smaller than in other oxide experiments, but still large enough to provide for a rapid cooling of the melt.

If a very thin sacrificial concrete layer is selected, the temperature of the melt is still extremely high when the water inflow sets in. In this case, the melt solidifies with a higher porosity and, hence, an increased volume flow of the cooling water. If water

inflow is delayed by a long erosion time of the sacrificial layer, as observed in experiment 8.2, the temperature of the melt is smaller. Here, the absence of decay heat as compared to the core melt becomes apparent. As a consequence, the starting water inflow leads to a smaller porosity of the melt, which is associated with a smaller volume flow rate. All crucible sections obtained from the oxide experiments show large cavities in the solidified melt, which are connected by smaller channels, and a cleaved and open melt surface, see Fig. 4.1.3. Hence, pure oxide melts can be cooled safely up to an initial height of 40 cm.

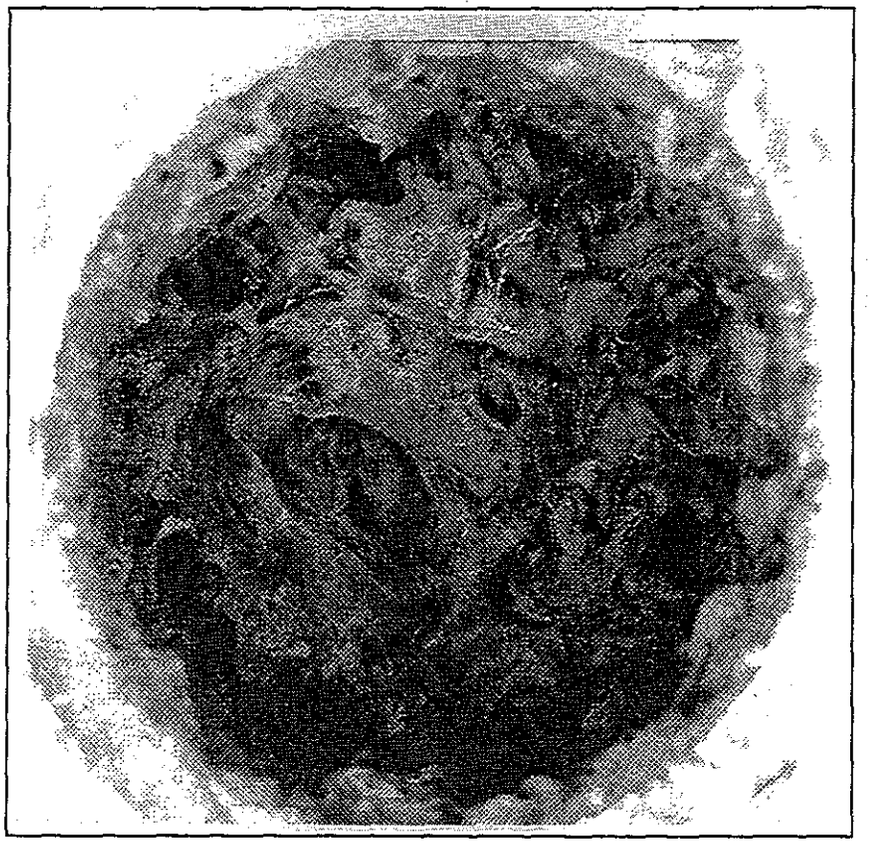

Fig. 4.1.3: **Top view of the porous solidified oxide melt**

Evaporation Rate and Heat Removal

The evaporation rates as obtained in the experiments 8.4, 8.5 and 8.6 from the difference between the inflowing water volume and the increase in weight of the test vessel are represented in Fig. 4.1.4. As the experimental conditions are the same except for the water pressure, these three experiments can be compared easily.

In the beginning, the inflowing cooling water is evaporated completely in all three experiments. Due to the high water pressure, the highest volume flow of nearly 400 ml/s is reached in experiment 8.4 about 30 s upon water inflow. Then, the melt is flooded slowly by the incoming water, the evaporation rate decreases and is practically zero after about 200 s. A very high value of 325 ml/s of evaporating water

is also reached in experiment 8.6 about 50 s after water inflow. This value then drops in analogy to experiment 8.4.

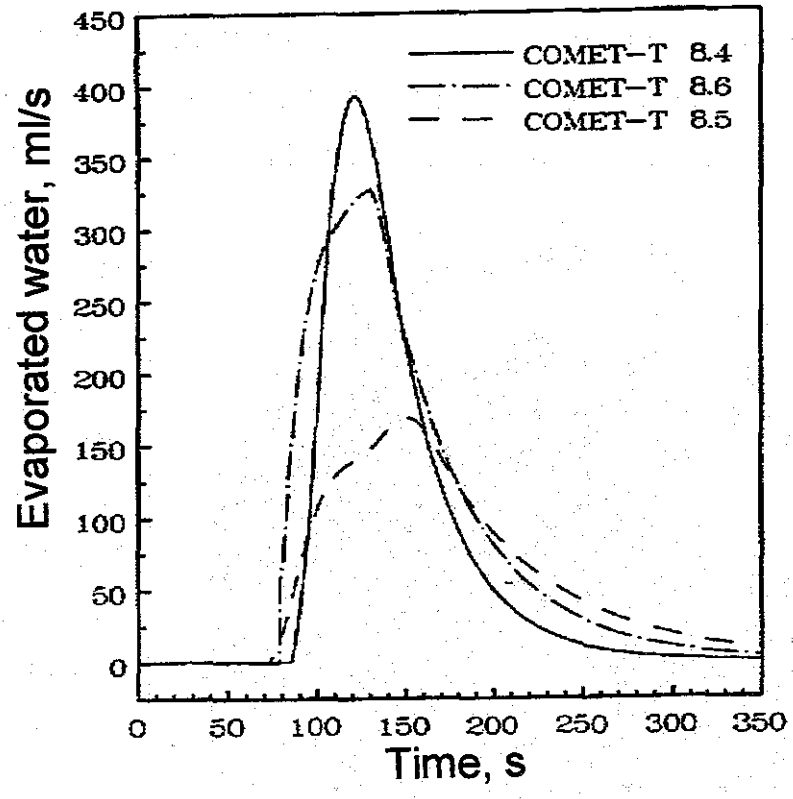

Fig. 4.1.4: **Comparison of the evaporation rates at various water pressures: Experiment 8.4 (0.4 bar), 8.5 (0.0 bar), 8.6 (0.2 bar)**

A different behavior is observed in experiment 8.5 at 0 bar water pressure. The maximum evaporation rate amounts to approx. 150 ml/s about 50 s after water inflow and, hence, is nearly half as high as the value in experiment 8.6. Due to the smaller incoming volume flow, however, the melt is cooled down more slowly, the evaporation rate decreases more slowly and still amounts to 25 ml/s about 200 s upon water inflow. The integral over the evaporation curve is about the same in all three experiments.

The heat removal rate is obtained from the evaporation rate multiplied by the evaporation enthalpy of the water. At a high pressure of the flooding water, maximum heat flow from the melt amounts to nearly 1 MW, but even in the experiment 8.5 at 0 bar flooding water pressure it still amounts to 400 kW. This is much more than is required to remove the decay heat and explains the rapid solidification of the melt.

For comparison, the temperature behavior of the melt as obtained from experiment 8.6 is represented in Fig. 4.1.5. The immersion probe with a W-R thermocouple is inserted into the melt about 60 s upon pouring of melt. After 90 s, the maximum value of about 1400 K is reached. This low value shows that the temperature of the melt has already been reduced by the starting water inflow. From the temperature reading of the immersion probe in the time interval of 125 - 160 s and the temperature drop of ΔT = 500 K, a temperature decrease rate of 14 K/s is obtained. This corresponds to a mean heat flow from the melt of 650 kW. This value is in good agreement with the heat flow removed to the incoming cooling water at this time, which is about 600 kW according to Fig. 4.1.4.

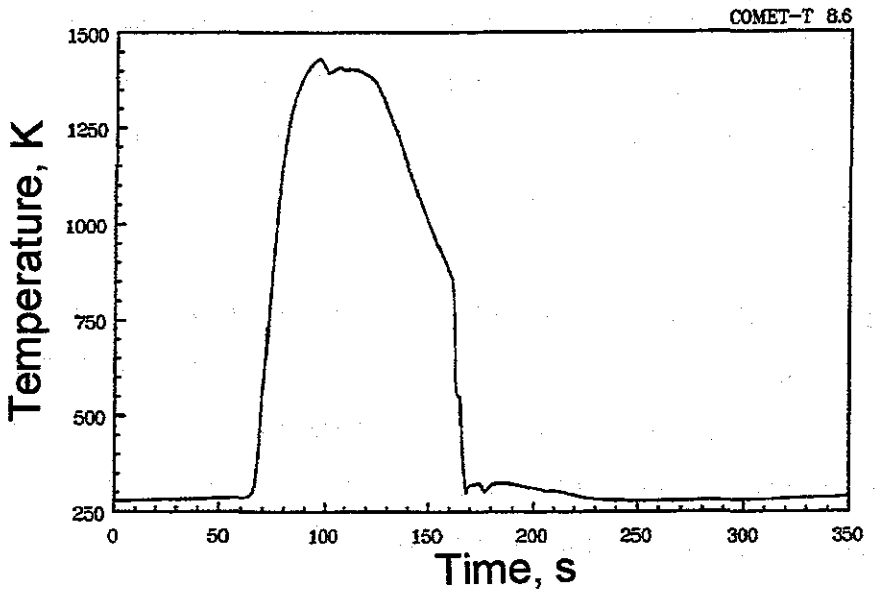

Fig. 4.1.5: **Temperature decrease in the melt in the interval of 125 - 160 s, as obtained by experiment 8.6**

Steam Explosions

When a hot melt is in direct contact with water, steam explosions are possible in principle. A steam explosion is understood to be the explosion-like evaporation of water by a very intensive mixing and heat exchange with a hot melt. This process requires a very fast fragmentation of the melt to a size distribution of the melt particles of millimetres or sub-millimetres within a period of a few milliseconds, and is driven by self sustaining shock waves in the fluid mixture. As also in the COMET core catcher concept water gets in direct contact with hot melt, the possibility of

steam explosions under typical cooling conditions and its maximum dimension and consequences have to be determined.

To provoke a steam explosion under the COMET cooling conditions and to quantify its consequences, a superheated melt was generated with significant water injection in the experiments COMET-T 2.1 and 2.3. This was established by a reduced height of the sacrificial concrete layer of 5 mm only and a water pressure of 0.2 and 0.4 bar.

Since erosion of the 5 mm sacrificial layer takes place rather rapidly, water inflow into the melt starts upon the completion of the thermite reaction after about 30 s already. The melt still has its high initial temperature resulting from the thermite reaction of about 2150 K. This value exceeds the solidification temperature by about 500 K. Furthermore, the flooding water pressure is selected to be sufficiently high to provide for a rapid water penetration into the melt and to establish an intensive contact between the melt and the water.

In experiment 2.1 at 0.2 bar water pressure, water inflow already starts after about 20 s. At first, it is accompanied by two rather vigorous melt/water interactions. It is demonstrated by force and pressure measurements, however, that both forces and pressures are relatively small and, hence, represent a small load only, although almost the entire oxide fraction is thrown out of the vessel.

In experiment 2.3 more vigorous interactions are expected due to the higher water pressure of 0.4 bar. Water inflow starts after 33 s. In the interval of 33-42 s, a total of six vigorous melt/water interactions take place, three of which exhibit maximum forces of up to about 10 kN (Figure 4.1.6).

The strongest impact can be noticed 41.1 s upon ignition or 8.1 s upon start of water inflow. Pressure measurements in the water supply line also reflect this event. The pressure increases to about 1 MPa differential pressure. From the time integral of the force curve, an impulse of $I = \int F dt = 76$ Ns can be determined.

The velocity at which the melt is hurled out of the vessel amounts to about 14 m/s. Momentum conservation yields a hurled-up melt mass of 5.4 kg with a kinetic energy of 530 J.

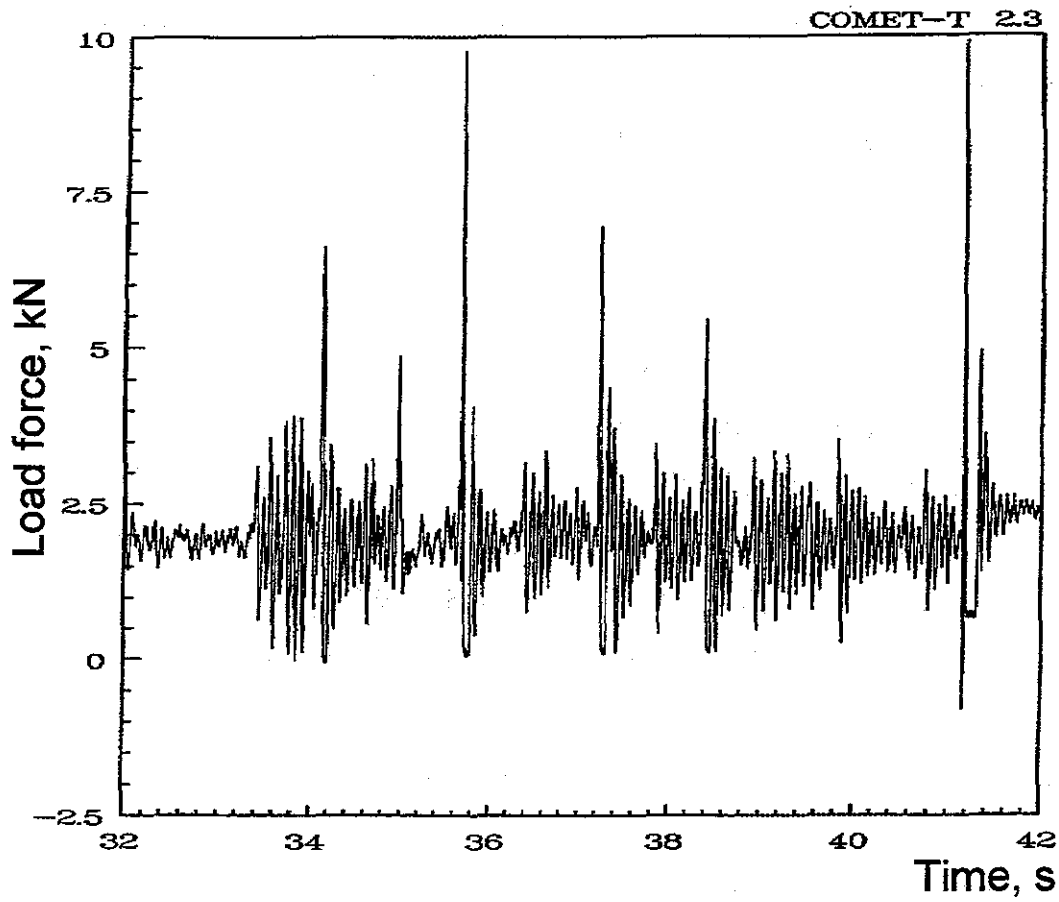

Fig. 4.1.6: **Force curve in experiment COMET-T 2.3: Vigorous melt/water interactions in the interval of 33 – 42 s**

The thermal energy contained in the entire melt is about 53 MJ. Consequently, a conversion efficiency of steam explosion of $\eta = E_{kin}/E_{therm} = 10^{-5}$ is obtained.

This value is so small, because of the small amount of water only that may penetrate into the melt via the open melting plugs and that is available for the interaction with the melt. Assuming that during the event observed about 5 cm^3 of water have penetrated into the melt via the melting plugs and reacted with the same volume of steel melt of 35 g, the local conversion efficiency can be derived. The steel mass of 35 g has a thermal energy of about 50 kJ as compared to the kinetic energy of 530 J obtained in the experiment. This yields a local efficiency of about 1% in the conversion of thermal into mechanical energy. Efficiencies of this order are also measured in steam explosion experiments. Consequently, the overall efficiency

which is smaller by three orders of magnitude in this experiment results from the limitation of the reacting amount of water.
Another important aspect for safety assessment related to this concept is the fact that larger amounts of water may accumulate only after the melt has cooled down considerably. For this situation, however, the risk of a steam explosion does no longer exist because the viscosity of the melt is significantly increased and crusts start to form.

In the 3rd experiment with a height of the sacrificial layer of 5 mm, no vigorous melt/water interactions are observed, as the effective water pressure amounts to 0 bar only. In the experiments performed with a height of the sacrificial layer of 10 mm, the melt cools down prior to water inflow such that vigorous melt/water interactions cannot be observed either. This suggests that steam explosions can be avoided in the COMET concept by an adequately selected height of the sacrificial layer to reduce the temperature of the melt prior to water contact.

Conclusions from transient thermite experiments

The following conclusions can be drawn from the transient cooling experiments with thermite melts:

- Both stratified metal and oxide melts as well as pure oxide melts are cooled down efficiently by water inflow from below.
- Averaged over all experiments of this test series, the porosity of the solidified metal melt amounts to 30%, whereas the respective value of oxide melt is 50%.
- The mean water inflow rate of more than 100 ml/s exceeds the rate required for cooling the core melt by one order of magnitude, as related to the spreading area of the cooling facility.
- Melts with an initial height of up to about 40 cm are cooled down rapidly and for a long term by water inflow from below due to the very efficient fragmentation process.
- The behavior of the pure oxide melts does not differ very much from that of the stratified metal and oxide melts as far as the coolability is concerned.

4.2 Experiments with Real UO_2-Containing Melts, COMET-U

The COMET-U test series performed at the ANL in Chicago (Ill), USA, are aimed at investigating the coolability of real corium melts with a high content of UO_2 as well as at evaluating the transferability of the experiments performed with iron-aluminum oxide simulation melts (thermite melts) to real corium melts [8]. The setup used for these transient COMET-U experiments therefore corresponds largely to that of the transient COMET-T experiments performed at the FZK and described in Sec. 4.1. Two experiments were carried out in a test vessel of 30 cm diameter, COMET-U1 with 110 kg corium melt and COMET-U2 with 150 kg corium melt. The height of the melt without void amounted to 30 and 40 cm, respectively.

The major constituents of the melt are 52% UO_2, 16% ZrO_2, 13% SiO_2, 4% CaO and 11% Cr. Hence, the composition of the oxide fraction corresponds to that of a core meltdown accident after the erosion of the sacrificial concrete layer. Nine melting plugs are integrated in the sacrificial concrete layer and connected with the water reservoir. In the first experiment, the nine plugs are covered by a concrete layer of 5 mm, in the second experiment by 15 mm. In analogy to the COMET-T experiments, these experiments are performed without reheating of the melt and, thus, cover the short-term aspects of cooling. The effective overpressure of the inflowing cooling water amounts to 0.1 bar in the first experiment COMET-U1 and to 0.0 bar only in COMET-U2.

The melt generated by the thermite reaction has an initial temperature of about 2500 K, see Fig. 4.2.1. The thermocouples in the lower part of the melt do not reach 2500 K, since part of the heat is removed to the cold concrete by the tungsten sheat of the thermocouples. At first, the melt has a very low viscosity. In the first experiment COMET-U1, the 5 mm thick sacrificial concrete layer is eroded within a few seconds with all nine cooling channels being opened and the passive water inflow setting in. Within 50 s, a practically stationary coolant water flow of 330 ml/s (20 litres per minute) is reached such that a very efficient cooling of the melt takes place (Figure 4.2.2). 4 minutes after water inflow already, the temperatures in the melt have dropped below 1400 K. Consequently, the melt has solidified safely in a

porous manner and the erosion of the sacrificial concrete is terminated. About 13 minutes upon water inflow, all temperatures show that the melt has cooled down completely as the temperatures are below 100°C. After 14 minutes, water supply to the test vessel is stopped by the operator.

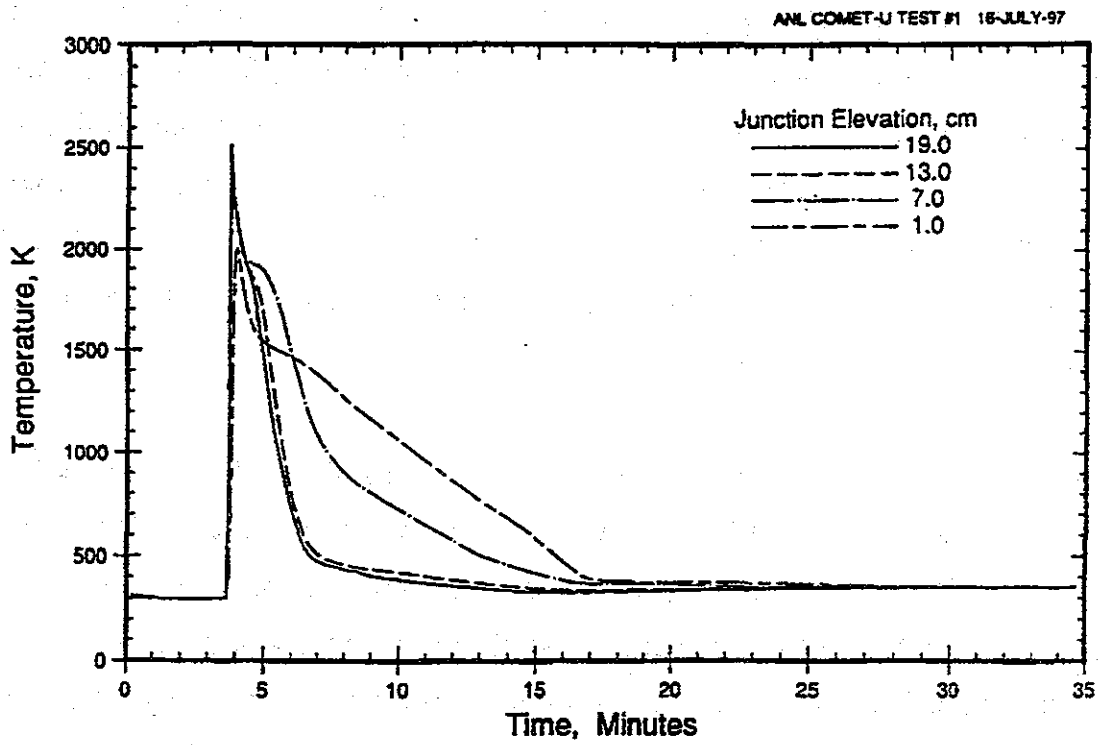

Fig. 4.2.1: **COMET-U1: Temperature behavior in the melt**

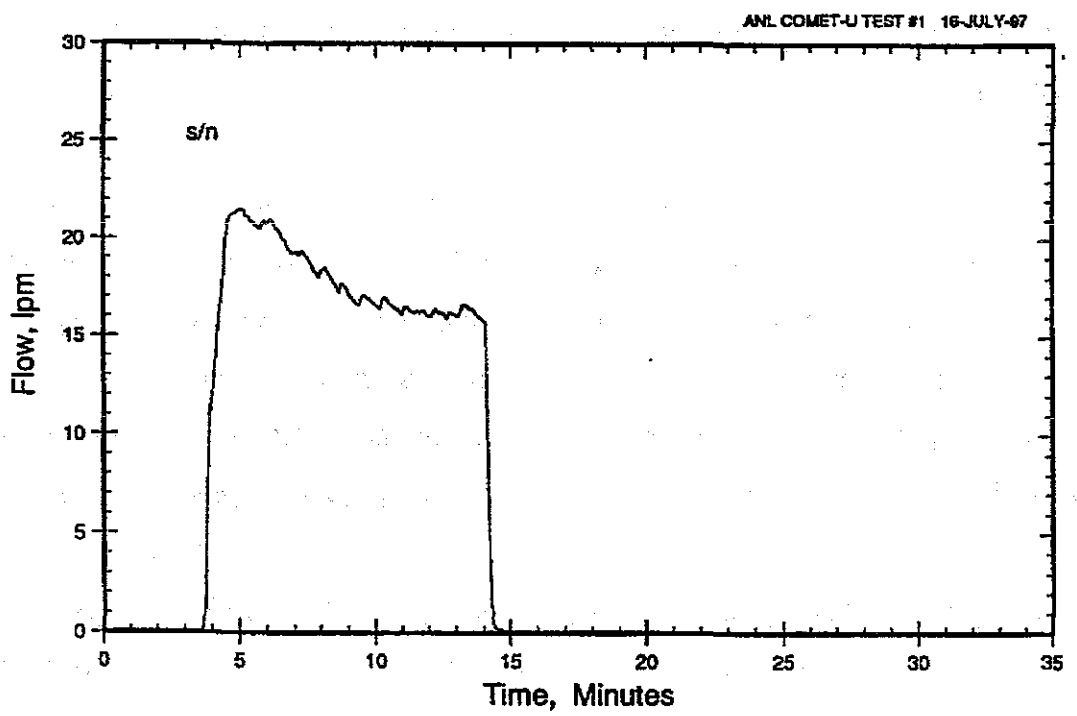

Fig. 4.2.2: **COMET-U1: Water inflow rate into the melt**

In the second experiment COMET-U2, because of the higher sacrificial concrete layer of 15 mm, the time for concrete erosion between the end of melt generation and the start of water inflow is extended until passive water inflow starts 1:00 min upon ignition. At first, water flow amounts to 120 ml/s and then increases to its maximum value of 220 ml/s (13 litres per minute) within 2 min. Afterwards, it remains practically constant, see Fig. 4.2.3. The water flow is interrupted by the operator after 17 minutes to limit the water level in the test vessel.

With onset of flooding the temperatures in the melt drop very rapidly with about 5-6 K/s (Fig. 4.2.4). About 1 min upon the start of cooling, the cooling rate is slowed down to about 1 K/s. The cooling phase then extends over a period of about 15 min. It is demonstrated by temperature measurements at the side walls and in the sacrificial concrete layer below the upper edge of the plugs that the surrounding structures remain cold. The temperatures of the base plate always remain below 50°C. Consequently, also this experiment reflects efficient cooling of the real corium melt even at a very low effective water pressure. In this case, the initial inflow rate of flooding water is favorably affected by gas release due to concrete erosion, as a result of which flow paths are generated in the melt.

The reduced water inflow as compared to the first experiment and the somewhat slower cooling of the melt are attributed to the smaller supply pressure of the flooding water. Comparison with experiments on Fe/Al_2O_3 thermite melts shows the same relative decrease in the flooding rate when the water pressure is reduced from 0.1 to 0.0 bar. This also means that the phenomena to be observed during the flooding of corium melts and simulation melts are the same.

During the flooding of the corium melt, maximum pressure fluctuations of 0.2 bar were measured. Hence, no vigorous interactions between the water and the melt occurred, s. Fig. 4.2.5. Post-examinations showed that all nine plugs had opened.

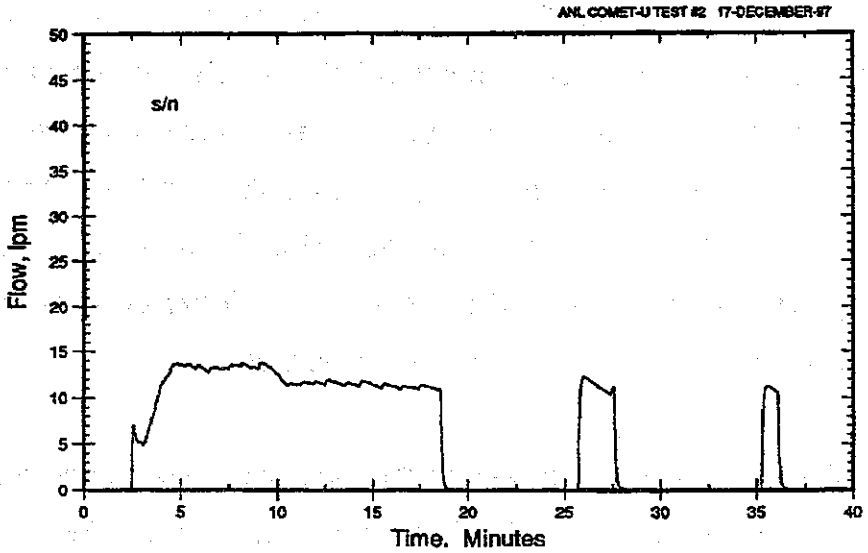

Fig. 4.2.3: **COMET-U2: Water inflow rate into the melt**

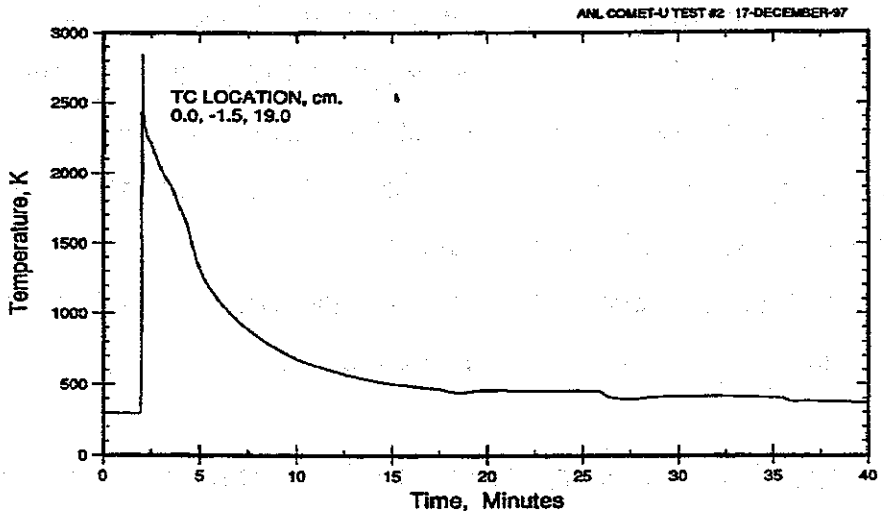

Fig. 4.2.4: **COMET-U2: Temperature history in the melt**

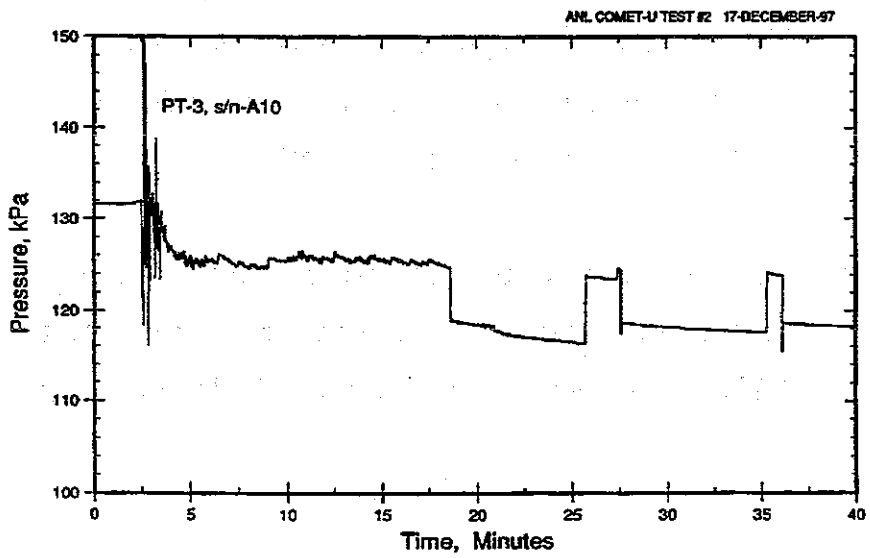

Fig. 4.2.5: **COMET-U2: Pressure behavior in the water supply line**

Conclusions

It is confirmed by both experiments that corium melts behave in the same way as the simulated corium melts applied in the experiments at the FZK. The water inflow from below causes the melt to fragment and solidify in a porous manner. The water inflow and cooling rates correspond to those measured by the FZK in the COMET-T experiments. The high water inflow rate ensures safe short-term and long-term cooling. Thus, the COMET concept is confirmed successfully also for the use of real melts.

4.3 Experiments with Sustained Heated Thermite Melts (COMET-H)

The COMET-H experiments (H denotes the heating of the melt during the experiment) are large-scale experiments performed with thermite melts of up to 1300 kg. Inductive heating of the melt at mean frequencies of 1000 Hz allows to simulate the decay heat generation in the melt with a power density that is characteristic of the real core melt. Simulation of heating extends from the beginning of the melt impact until complete solidification and beyond [5]-[8].

The experiments represent a one-dimensional, 92 cm diameter circular section of the large cooling facility. The geometrical heights, including the heights of the melt, correspond to the real setup. As also the melt temperatures and properties largely correspond to those of a real core melt after partial erosion of the sacrificial layer, the characteristic heat fluxes and solidification processes during cooling are represented practically 1:1. The melts possess a metal fraction, above which a layer of the lighter oxidic melt is located. They are generated by an iron-thermite reaction under the addition of further components at temperatures of about 1900°C and poured onto the cooling area. The metal melt with a mass fraction of about 50% consists of iron with a representative amount of zircaloy added depending on the objective of the experiment. The oxide melt consists of a mixture of aluminum oxide and calcium oxide, the major properties of which correspond to those of the uranium/zirconium oxide melt mixed with molten concrete in the real reactor. For the verification of the results obtained with these experiments, the COMET-U experiments with uranium-rich melts were performed (Section 4.2). Thus, the suitability of the cooling device for real melts was confirmed.

The COMET-H experiments are designed such that a typical power of 300 kW is generated continuously in the melt. The cooling area is 92 cm in ∅. This corresponds to a surface power density of 450 kW/m^2, and therefore represents the highest level of decay heat that have to be managed in the EPR. Inductive heating of the melt takes place by means of a flat induction coil that is arranged below the cooling facility, see Fig. 4.3.1. The power is generated in the metal melt and transferred to the oxide phase by conduction and convection. The advantage of

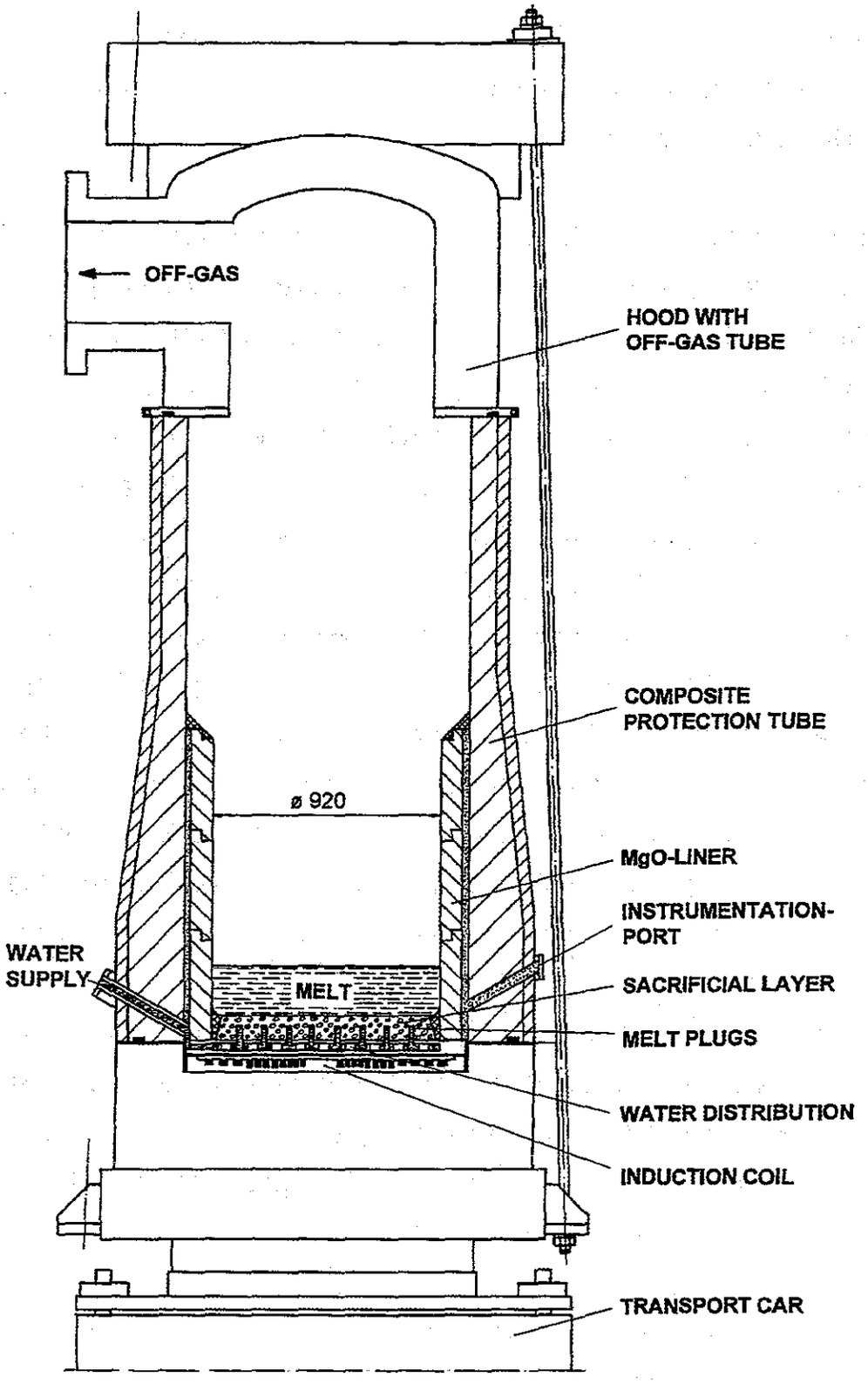

Fig. 4.3.1: **COMET-H Test Facility with Sustained Heating**

inductive heating as compared to other heating methods is that it can also be maintained during and after solidification. After solidification, however, the simulation of decay heat is mainly restricted to the metal phase, as heat transfer to the oxide by conduction alone is rather small.

The cooling insert above the induction coil is usually equipped with 112 water-conducting melting plugs/cooling channels, arranged in a square grid of 8 cm. As of experiment COMET-H 2.2 upwards, these plugs are imbedded into a 5 cm high layer of castable aluminum oxide with a view to improve the stability against downward melting. This layer is covered by the sacrificial layer of concrete that is produced on the basis of borosilicate glass. Both layers are equipped with thermocouples at various levels, which provide information on the progress of erosion and the cooling state of the melt. Glass fiber-optical waveguides are applied as safety-related instruments: Disruption by the hot melt causes them to automatically switch off the induction heating. The carrier construction of the cooling insert is made of epoxide resin, since inductive heating does not allow the use of metal materials. Failure of the plastic would occur at about 300°C in case that fast quenching of the melt would not be achieved. Of course, in the reactor a steel construction would be applied as its thermal robustness is higher. Flooding water is supplied from an elevated tank to the four segments of the water distribution layer and to 10 individual melting plugs. This allows a statement to be made with regard to the homogeneity of the water flow to the melt. In addition to the temperatures mentioned above, the inflow of coolant water and its pressures are measured. Furthermore the temperatures, volumes, pressures and compositions of the exhaust gas flows are determined. Video monitoring in the crucible allows rather important findings be obtained with regard to the state of the melt and the efficiency of cooling.

Figure 4.3.2 shows the cooling facility with the melting plugs prior to the application of the sacrificial concrete layer.

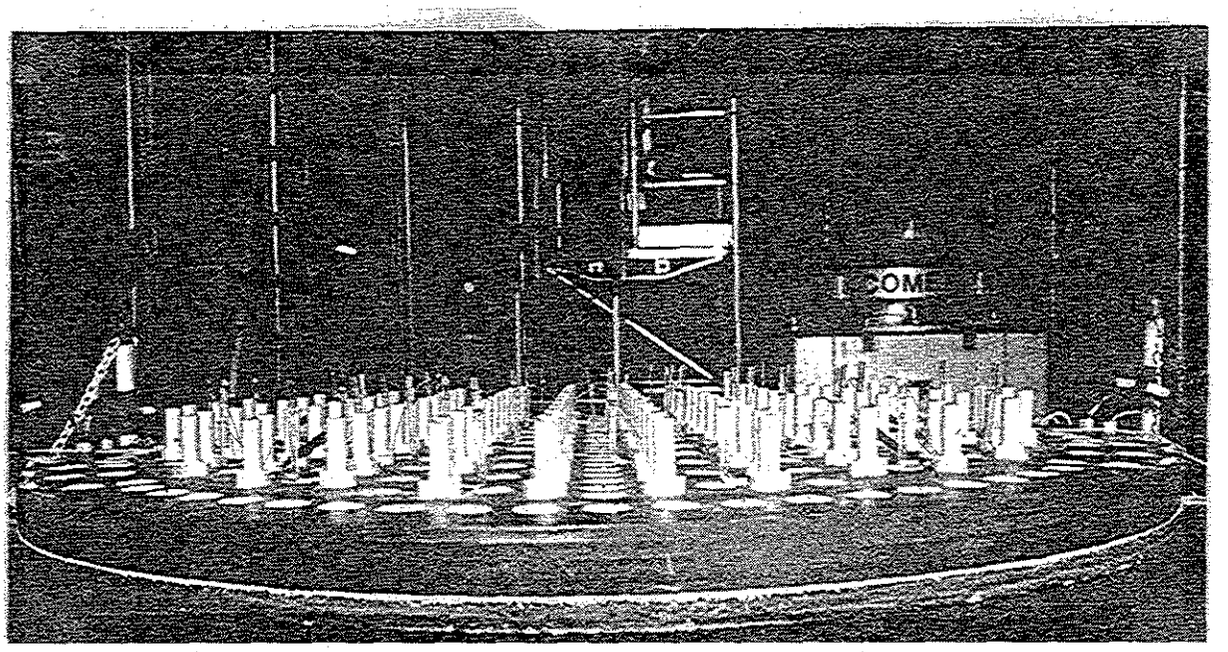

Fig. 4.3.2: **COMET cooling facility with melting plugs/cooling channels prior to the pouring of the sacrificial concrete layer**

Test Matrix

From 1995 to 1998, 10 COMET-H experiments were performed. They are presented in Table 4.3.1. After qualification tests of the large scale facility, the experiments COMET-H 1.x first concentrated on safe cooling under normal conditions at an effective overpressure of the cooling water of 0.2 bar. The melt masses were increased to 800 kg with a height of the melt of up to 32 cm. The COMET-H 2.x test series served to investigate cooling in the case of a inhomogeneous erosion of the sacrificial concrete layer and led to the application of the ceramic sublayer as of experiment COMET-H 2.2. The first two experiments of the COMET-H 3.x test series were performed to study the effect of metallic zircaloy on cooling. The two last experiments, with COMET-H 3.3 providing no information on the coolability due to the early failure of the decay heat simulation, focused on the analysis of extreme EPR conditions with a very high melt and a low water pressure of 0.1 bar.

Table 4.3.1: **COMET-H experiments with sustained heated melts (1995-98)**

Experiment	Objective	Result
COMET-H 0.1 January 28, 1995	Commissioning test, 300 kg melt	Successful with short-term induction heating
COMET-H 1.1 July 8, 1995	Standard geometry, 500 kg, H = 19 cm	Cooling achieved, induction heating is not yet sufficiently stable
COMET-H 1.2 November 18, 1995	Standard geometry, 650 kg, H = 25 cm	Safe cooling, long-term cooling is demonstrated
COMET-H 1.3 April 20, 1996	Standard geometry, 800 kg, H = 32 cm	Safe short-term and long-term cooling under sustained heating
COMET-H 2.1 October 12, 1996	Influence of inhomogeneous erosion 650 kg, H = 26 cm	Penetration of small amounts of melt into the bottom water layer
COMET-H 2.2 March 8, 1997	Influence of inhomogeneous erosion 650 kg, H = 26 cm	Ceramic base layer ensures coolability
COMET-H 3.1 June 28, 1997	Influence of Zr metal, 885 kg, H = 34 cm	At first complete Zr oxidation during concrete erosion, then water inflow with complete cooling
COMET-H 3.2 November 29, 1997	Influence of Zr metal, reduced water pressure with modified plugs	Sufficient amount of flooding water, but penetration of small amounts of metal into the bottom water layer
COMET–H 3.3 May 9, 1998	Extreme EPR conditions with 1300 kg (low water pressure, high melt)	After start of cooling failure of decay heat simulation, experiment is not valid as far as cooling is concerned
COMET–H 3.4 July 11, 1998	Repetition of COMET-H 3.3	Strong local erosion of the sacrificial layer; in spite of a sufficient cooling water flow, about 18 kg of not yet solidified metal melt penetrates into the water layer after 45 minutes

Of the eight experiments, in which the decay heat was simulated successfully (not simulated in H 0.1 and H 3.3), six experiments ended with a complete coolability and a completely solidified melt. In experiment H 2.1, aimed at studying the consequences of a locally increased erosion of the sacrificial concrete, a part of the melt penetrated through the sacrificial concrete layer and the plastic carrier plate while the fragmentation of the melt was still ongoing and thus, entered the bottom water layer. Consequently, the ceramic base layer was introduced to improve the stability. In experiment H 3.4, application of extreme test parameters (high melt at low water pressure) indicated the limits of safe operation, as - due to insufficient flow through the cooling channels - the still liquid residual melt penetrated into the water layer late in the test.

The major results of these experiments shall be presented below. Some characteristic values of the experiments are listed in Table 4.3.2.

Concrete Erosion and Start of Cooling

In all experiments, the melt is poured onto the cooling facility from a height of about 2.5 m as a free falling jet. The melt immediately spreads on the surface. The directly starting gas release from the concrete prevents a strong local erosion near the point of impact of the jet. The initial temperature of the melt varies between 1640 and 1900°C depending on the experimental conditions.

In all experiments, the erosion of the sacrificial concrete layer is determined by the bottom metal layer. The erosion rate is highest immediately after the pouring of the melt. Due to the decreasing temperature of the melt, however, it is rapidly reduced to a nearly constant value which is determined by the decay power simulated in the melt. Assuming that a decay heat power of 450 kW/m^2 is completely converted into concrete erosion, the approximate stationary erosion velocity v upon the decline of the first rapid erosion is derived as:

$$v = N_A / (\rho \cdot \Delta h).$$

Here N_A is the decay heat power/m^2 = 450 kW/m^2, ρ is the density of the concrete = 2270 kg/m^3 and Δh is the decomposition enthalpy of the concrete = 2.1 MJ/kg. This yields v = 0.094 mm/s as an upper limit for the long term erosion velocity.

Table 4.3.2: Results of the COMET-H experiments

COMET-H		1.1[1]	1.2[1]	1.3[2]	2.1[3]	2.2	3.1[4]	3.2[4]	3.3[5]	3.4
Melt mass	m_0, kg	500	650	800	650	650	885	845	1295	1294
Melt height	h_0, cm	19	25	32	26	26	34	33	50	50
Melt pouring temperature	T_0, °C	1825	1710	1880	1690[6]	1640[6]	1900	1900	1700	1680
Effective water pressure	Δp, bar	0.2	0.2	0.2	0.2	0.2	0.2	0.1	0.1	0.1
Height of sacrificial layer	Δs, mm	50	50	50	80/110	80/110	110	110	110	110
Erosion rate	$\bar{v}_{max}$, mm/s	0.19	0.17	0.42	0.11/0.079	0.073/0.079	0.25	0.16	0.22	0.15
Start of water inflow	Δt, s	265	300	120	745/1400	1102/1400	434	702	495	720
Water inflow rate	V_w, l/s	1.3	0.25	2.0	0.85	1.2	1.9	1.3	0.12	1.0
Maximum heat removal	$N_{D,max}$, MW	1.2	not determined	not determined	1.9	1.9	4.2	3.0	0.8	2.5
Time until surface flooding	Δt_F, s	800	900	500	1800	1560	700	1020	1500	1200
Complete cooling		yes	yes	yes	no	yes	yes	yes	not applicable	no
Amount of hydrogen	m_{H2}, g	310	420	540	620	670	2400	1300	1200	1300
Molar ratio	$H_2/H_2O_{concrete}$	0.36	0.48	0.62	0.36	0.39	1.25	0.70	0.65	0.70

1 Mean heating power of 200 kW only
2 Sacrificial concrete made of spherical HAW glass aggregate
3 Number of melting plugs halved with 113 mm mesh width
4 Zircaloy as constituent of the metal melt
5 Termination of the test due to failure of induction heating
6 Expected temperature 1900°C, thermite reaction probably incomplete

Actually, the penetration of the melt downwards does not take place homogeneously of the entire area, but certain local fluctuations can be observed, which also cause the various melting plugs to open over an extended time period.

The time intervals from the pouring of the melt until the opening of the first melting plug are listed in Table 4.3.2. They correspond to the minimum erosion time of the sacrificial layer of the height Δs above the plugs. A maximum erosion rate $\bar{v}_{max}$, relative to the area and averaged over time, is assigned to this value. Due to the initially high temperature of the melt, this mean value is expected to be higher than the values that would occur under stationary conditions. Depending on the experiment, the measured erosion rates vary between 0.073 and 0.25 mm/s. In view of the fact that the higher erosion rates are measured in experiments with a considerable zircaloy fraction, as a result of which erosion is accelerated significantly, their agreement with the stationary estimate of 0.094 mm/s is reasonable.

The very high erosion rate in the experiment COMET-H 1.3 of 0.42 mm/s, however, has another reason. In this experiment, the sacrificial layer was made of a borosilicate aggregate of glass spheres and not of broken glass as in the other experiments. Obviously, this glass concrete has a much smaller resistance against the attack of the melt, because the glass spheres are not fixed mechanically into the cement matrix and may therefore detach at lower temperatures already. This undesired behavior may be avoided by an appropriate concrete production method.

In accordance with the initially higher erosion rate, large amounts of steam are released during concrete erosion at first. They pass the melt in a strongly turbulent manner and may tear up the melt surface and hurl up parts of the melt. Part of the steam may react chemically with the metal melt, as described below. Within 2 to 3 minutes, this phase changes to a calmed-down erosion phase which is mainly characterized by the equilibrium of decay heat power and removed thermal power. If considerable fractions of zircaloy are contained in the melt (COMET-H 3.1 and 3.2), the phase of intensive melt bath agitation due to the energy introduced from the strongly exothermic Zr oxidation is extended.

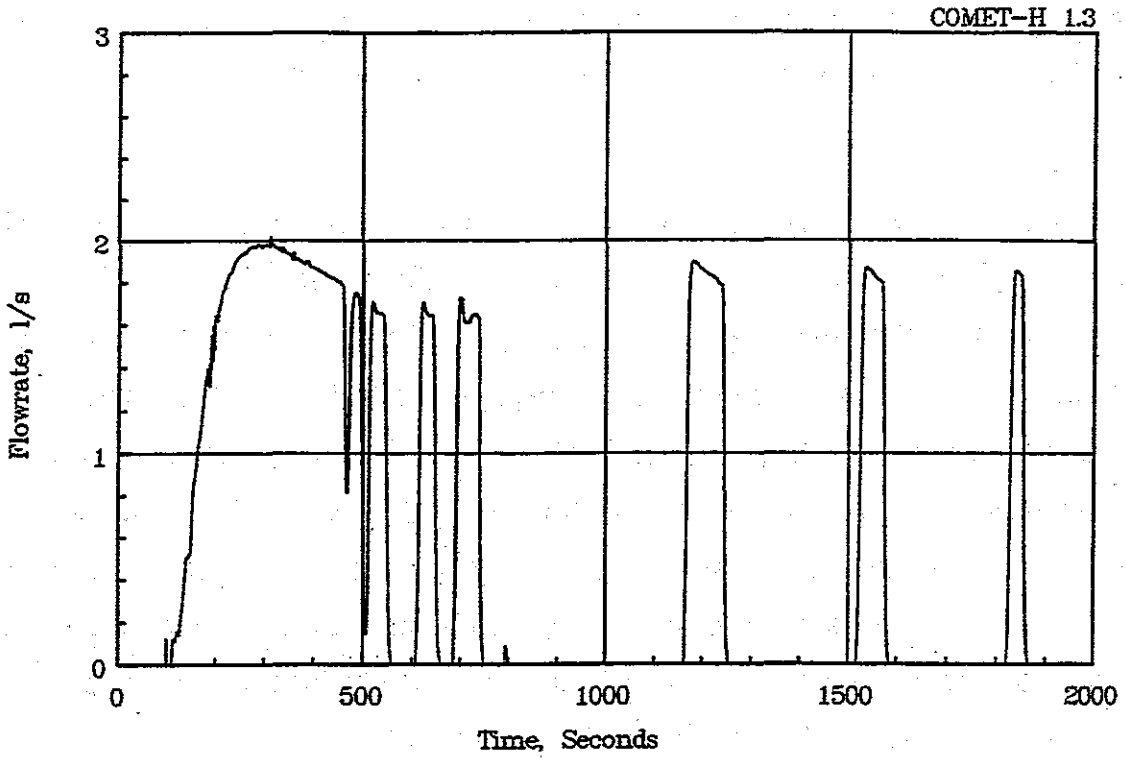

Fig. 4.3.3a: **COMET-H 1.3, inflow of cooling water into the melt**

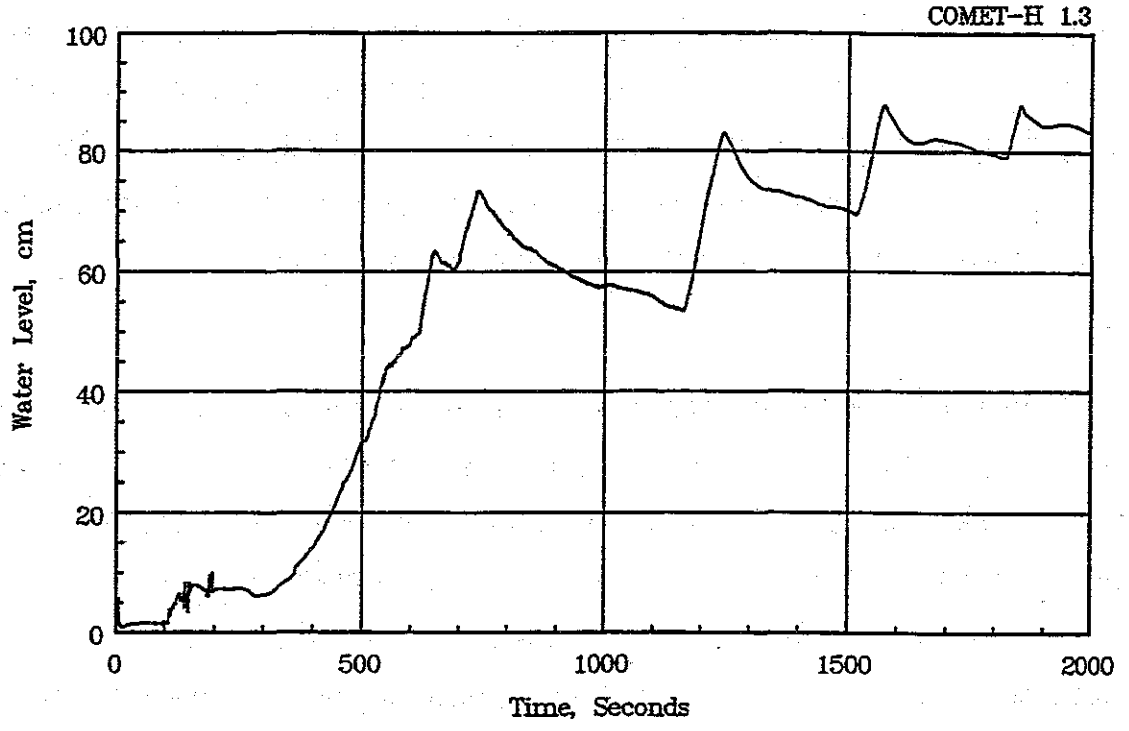

Fig.4.3.3b: **COMET-H 1.3, approximate level of cooling water in and above the melt**

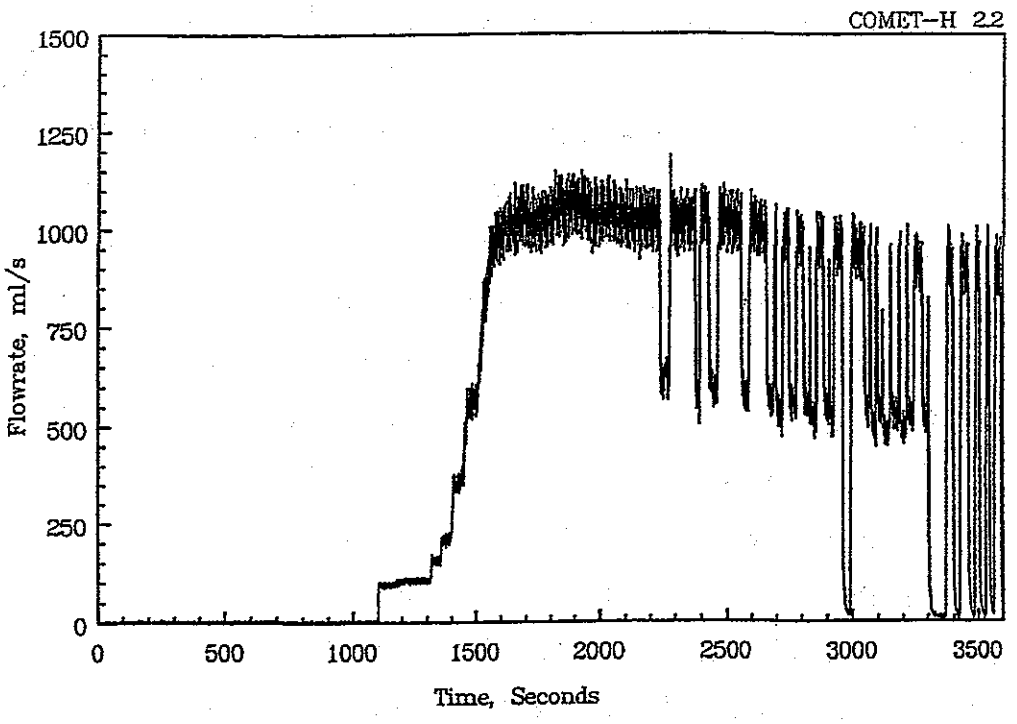

Fig. 4.3.4a: **COMET-H 2.2, inflow of cooling water into the melt**

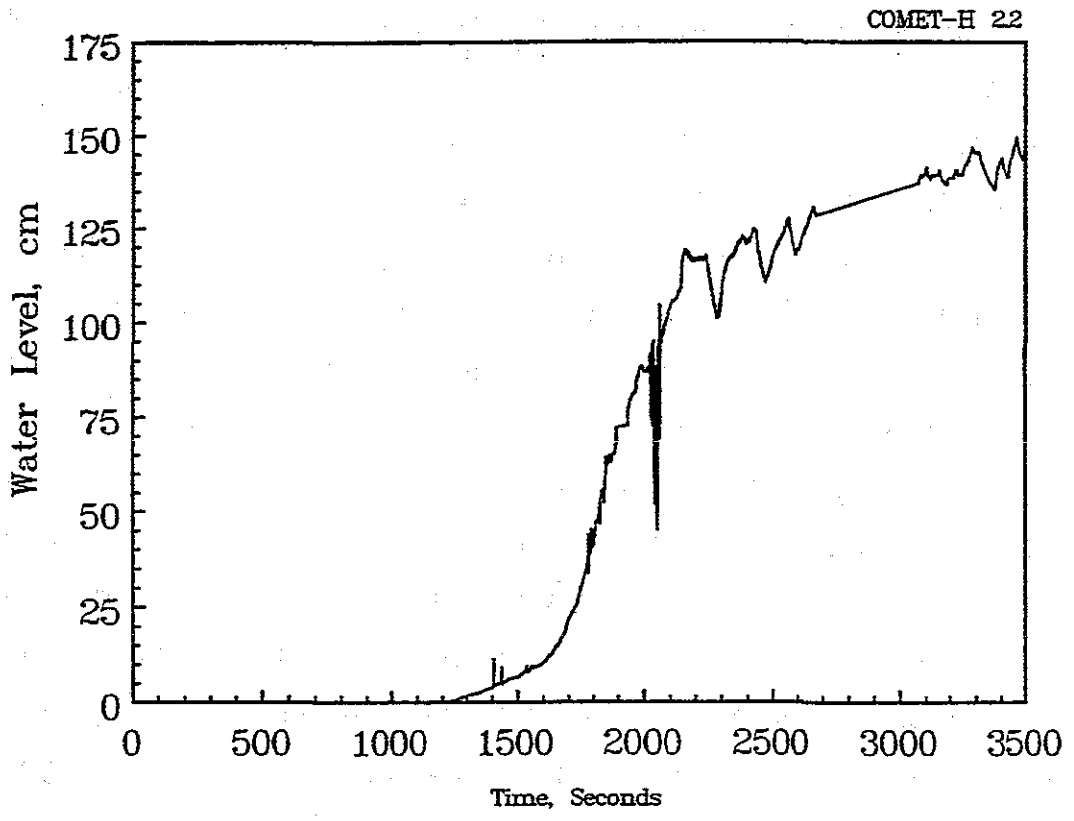

Fig. 4.3.4b: **COMET-H 2.2, approximate level of cooling water in and above the melt**

When the first cooling channels are opened by the ignition of the burnable caps, passive flooding of the melt from below starts. Fig. 4.3.3a shows the flooding process in COMET-H 1.3 for the case of a high number of cooling channels opening rapidly. According to separate measurements of the inflow rates, the channels open in the interval from 120 to 180 s, i.e. within a period of 60 s only. The number of open channels of 75 is very large in this experiment, as the sacrificial concrete has been eroded rather easily, as mentioned above. This experiment therefore represents the boundary case of a very rapid transition to a flooded melt. Following the flooding of the melt surface, water supply was interrupted several times after 450 s in order to limit the water level in test vessel. The approximate water level in/above the melt is shown in Fig. 4.3.3b. It is evident that the water level only starts to rise after the water has penetrated for a longer period of time. This means that boiling water only starts to rise from below in the solidifying melt after the melt has cooled down considerably following the initially complete evaporation of the penetrating water.

Another boundary case of water supply is shown in Fig. 4.3.4a, as obtained by the experiment COMET-H 2.2. Here, an inhomogeneous erosion of the sacrificial concrete with a local start of flooding was simulated by using melting plugs of variable length. In accordance with the experience gained from the previous experiment, the sacrificial concrete layer had been supplemented by a ceramic base layer in order to achieve a sufficient stability of the cooling device against the attack of the melt for the duration of the longer cooling process. Local flooding starts at the time of 1192 s with a small water flow only. At first, only the melt near the open cooling channels is cooled down. This small cooling water flow rate of 0.1 l/s is observed over a period of some 200 s, during which a part of the melt surface solidifies, but concrete erosion proceeds further by the not yet cooled sections of the melt. Then, further cooling channels open and water inflow and, hence, the cooling of the melt are improved steadily. An enlarging surface crust develops and finally the melt surface is flooded. Another major cooling and fragmentation process observed during this phase is the multiple break-up of the surface with the formation of volcanoes, through which glowing particles are ejected from the melt, enter the water, and freeze. These processes which result in improved cooling are associated with the opening of further plugs and completed after about 1800 s (see water level in Fig. 4.3.4b). Then, the

melt is completely solidified, and the decay heat is removed in a stable manner. Water supply amounts to 1.0 l/s, the number of open plugs is 22.

It is demonstrated by this experiment that locally starting cooling is improved by the opening of further cooling channels in the adjacent areas until the melt is stabilized and cooled down completely. The opening of the channels takes place over a period of 700 s. During this phase, surface crusts which form by water flowing onto the surface of the melt, are broken up in case of insufficient cooling of the melt from below. This also applies to crusts which form and stabilize at the edge of the test vessel of 92 cm in diameter. Sometimes small volcanoes are formed, the driving pressure of which is generated by the water penetrating and evaporating from below. These volcanoes promote the further fragmentation of the melt.

In all experiments with a successful simulation of decay heat, cooling water flow into the melt was significantly higher than 0.125 l/s, which is sufficient for the decay heat to be removed by evaporation of the cooling water. Therefore, cooling is ensured if the fragmentation and the water flow through the melt are sufficiently homogeneous. Incomplete cooling which was observed in experiment COMET-H 3.4 shall be dealt with below when presenting the limits of coolability.

Pressure Events during Water Inflow from Below

When the cooling water comes into contact with the hot melt, a rapid evaporation starts, which may turn into a steam explosion under extreme conditions as described in Chapter 4.1. However, no steam explosions were observed in the COMET-H experiments, which is mainly due to the limitation of the water supply via the cooling channels.

With respect to pressurization, the experiment COMET-H 1.3 represents the most critical case, as here the cooling water penetrates very rapidly into the still very hot melt. Figure 4.3.5 shows that no marked pressure peaks (< 0.1 bar) occur under these conditions. This applies to both the water supply and the gas plenum above

the melt. As a result of the rapid evaporation, however, parts of the melt are hurled upwards.

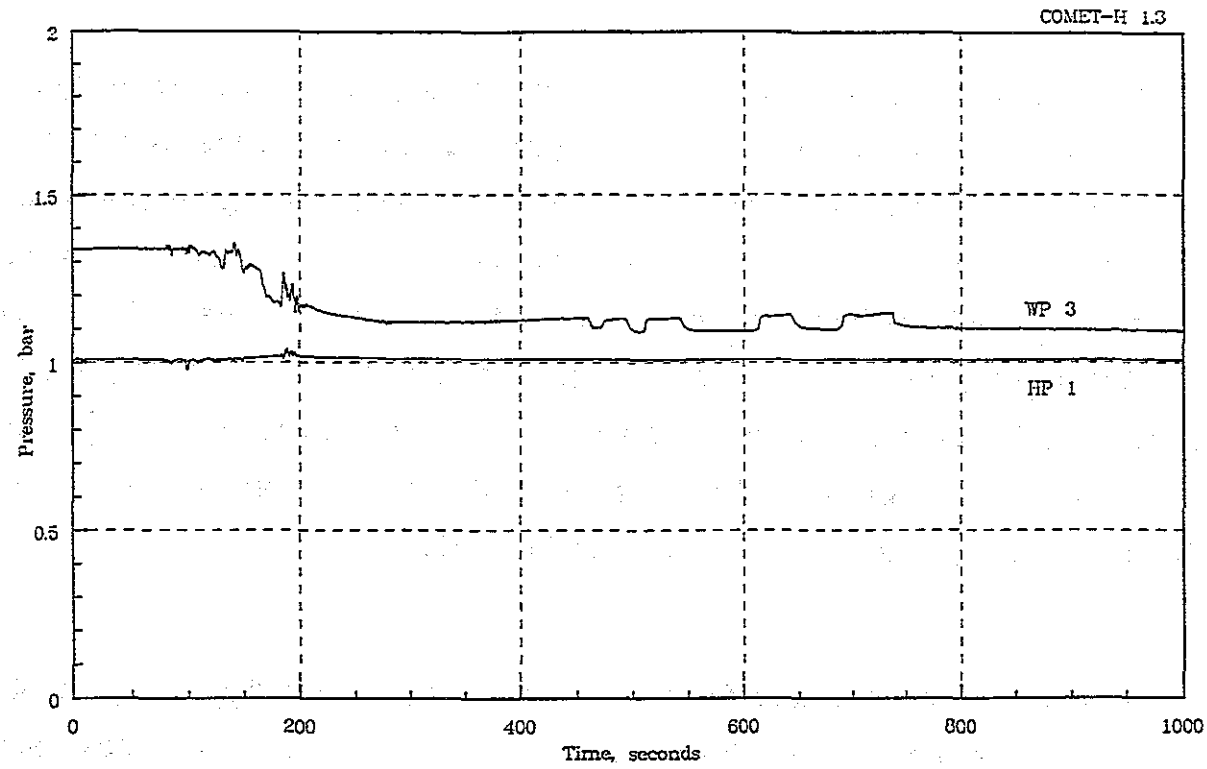

Fig. 4.3.5: **Pressure history during water inflow as measured in the COMET-H 1.3 experiment for the water supply (WP3) and the gas plenum above the melt (HP1)**

Heat Removal from the Melt and Comparison with the Decay Heat Production

By measuring the temperature and volume flow of the escaping steam, the heat removed from the melt after water inflow is determined quantitatively in the COMET-H experiments. The diagrams obtained from three significant experiments in Fig. 4.3.6 show the cooling behavior versus time in comparison with the decay heat power simulated in the experiments. Experiment COMET-H 3.4 is also taken into account. In this experiment, part of the melt was not cooled down sufficiently and entered the water layer at 2700 s. The behavior of the cooling rate is very similar in all experiments. The increase in the cooling rate reflects the inflow rate of the flooding water with a complete evaporation and a subsequent overheating of the steam rather well. The cooling rate considerably exceeds the decay heat production of the melt. With the proceeding cooling of the melt, it decreases continuously until the decay heat

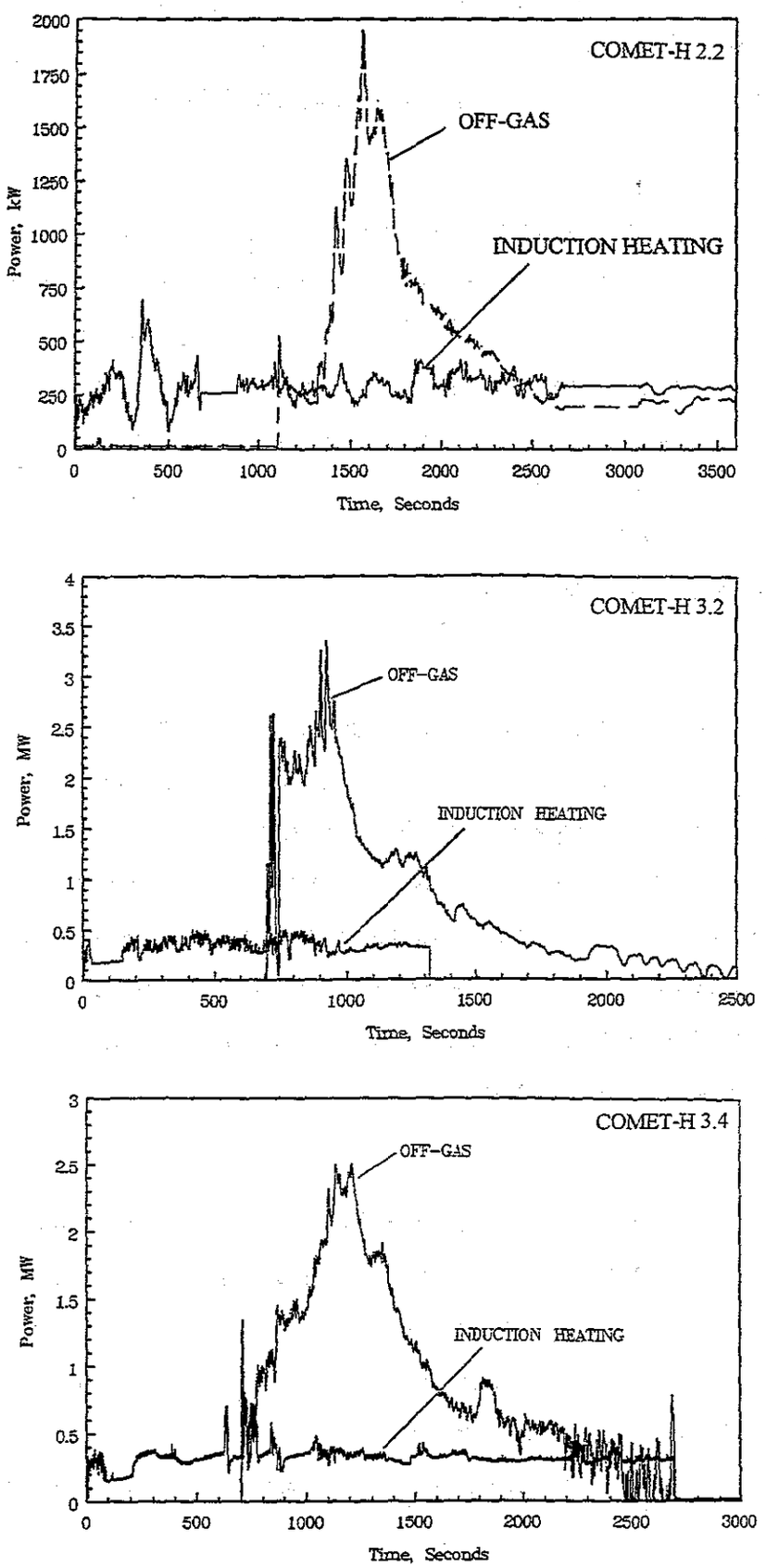

Fig. 4.3.6: **Heat removal from the melt by the steam flow in comparison with the simulated decay heat power, experiments COMET-H 2.2, 3.2 and 3.4**

level is reached. This moment depends on the mass of the melt and the energy contained therein, but typically is 1000 s upon the beginning of cooling. Accordingly, the water level in the melt rises during this period, as the water inflow rate is higher than its evaporation. During this time, solidification of the melt is completed.

In comparison with the transient test reported in Section 4.1 and 4.2, the sustained heated tests show the same phenomena during cooling: With onset of bottom flooding the characteristic cooling and fragmentation processes start with heat fluxes extracted from the melt up to a few MW per m^2 of the base cooling surface. But the larger and – as related to the reactor situation - characteristic height of the melt in the COMET-H tests and some lateral incoherences in the cooling processes on the larger surface, as well as the sustained decay heat simulation result in a longer time period for the melt to solidify.

In table 4.3.2 above the maximum heat removal measured for the different experiments is included. In experiments 3.1 and 3.2, this value reaches 4.2 and 3.0 MW, respectively, and, hence, is very high. This is attributed to the fact that 80 and 40 kg of zircaloy, respectively, have been added to the melt and that their oxidation enthalpy contributes to the energy balance. In the other experiments, the maximum values amounted to 1.0 - 2.5 MW, which corresponds to 1.5 - 3.8 MW/m^2. This value is higher than the heat that has to be removed due to the decay heat generation of max. 0.45 MW/m^2 by a factor of 3.

By integrating the cooling rates over time in Fig. 4.3.6, the energy removed from the melt is obtained. The above measurements show that the removed energy largely corresponds to the initial energy of the melt when poured into the test crucible plus the decay heat added during the experiment. The chemical energy resulting from the exothermic Zr oxidation and the endothermic chemical decomposition of the cement stone in the concrete max be neglected for this simple energy balance.

Porosity of the Solidified Melt and Long-term Cooling

For a good coolability of the melt, the porous structure which is formed during cooling and solidification of the melt is of primary importance. Fig. 4.3.7 shows the structure of the melt by the example of two sections obtained from the experiments COMET-H 1.3 and H 2.2. The solidified metal melt has a typical porosity of 30%, whereas that of the oxide is higher than 50%. The free surface of the oxide is always cleaved and has a number of openings, through which the cooling water may penetrate.

The higher porosity of the solidified oxide is explained by its increased viscosity in the vicinity of the solidification zone. On the other hand, the metal possesses a good coolability due to its improved thermal conductivity even in case of a smaller porosity. Hence, cooling of the metal was successful in nearly all COMET experiments, although the decay heat production in the metal layer was higher than it will be in a core meltdown accident.

In the experiments with insufficient cooling (COMET-H 2.1 and H 3.4), water inflow through the cooling channels to the lower side of the metal layer was not sufficient in certain areas. The reason shall be discussed below under the heading of "limits of coolability".

The carrying structures of the cooling facility and its surroundings remain cold, as they are in contact with the cooling water. Their temperatures are limited to about 100°C. This also applies to the ceramic base layer which carries the solidified melt. This is confirmed by the measurements performed in the experiments with decay heat simulation in the phase following the complete solidification of the melt. Here, the porous solidified melt is flooded and covered by water, while the decay heat is removed by stationary boiling.

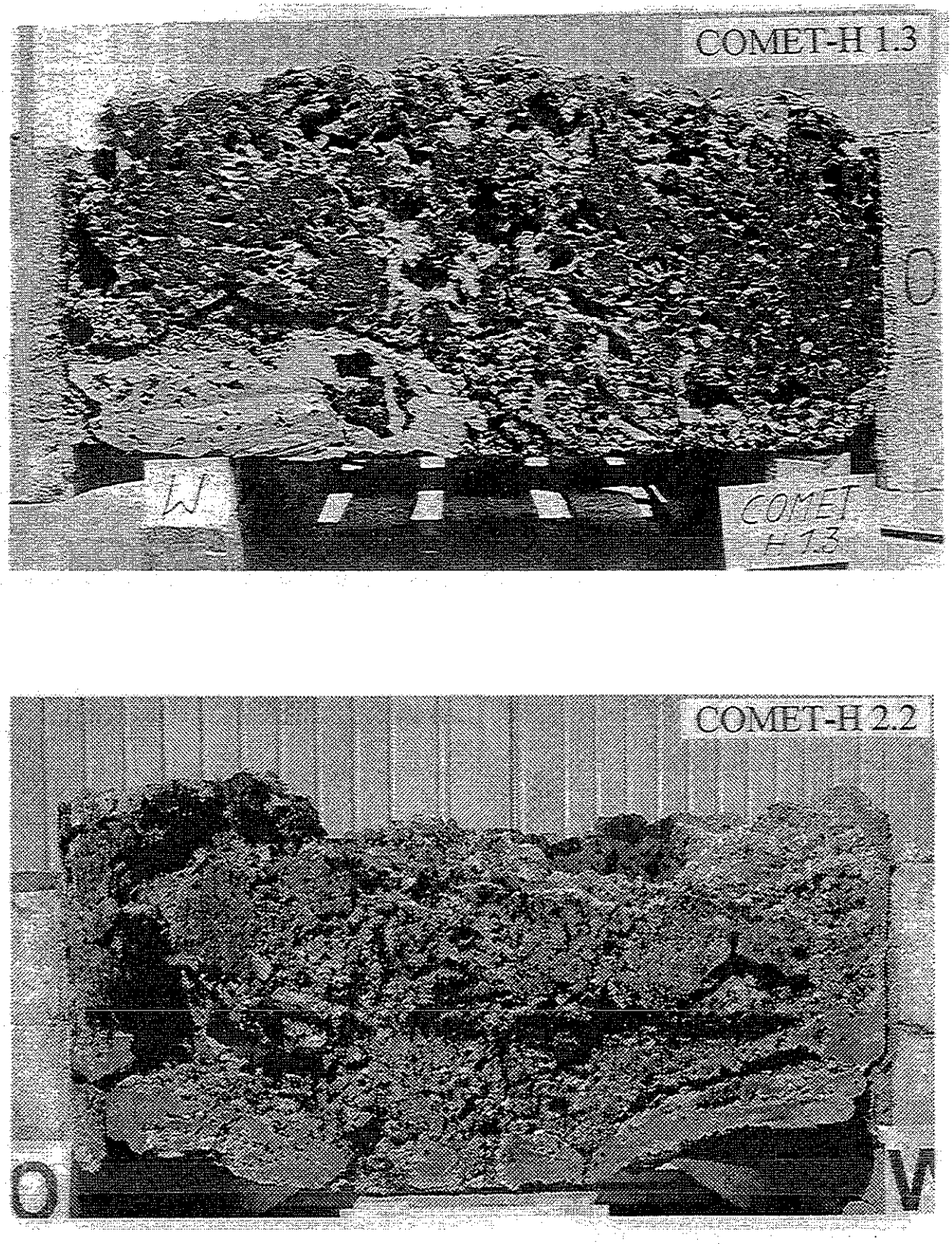

Fig. 4.3.7: **Porous solidified melt as obtained in the experiments COMET-H 1.3 and H 2.2**

Chemical Reactions and Hydrogen Release

During concrete erosion and at the onset of cooling, chemical reactions with the melt take place. If no zircaloy metal exists in the melt, the major reaction is that of iron metal with the steam that passes the melt as a result of concrete decomposition and flooding. The metal is partly oxidized and free hydrogen is generated. The reaction is stopped when the metal melt solidifies.

In most COMET-H experiments the reaction with Fe is important. Exceptions are COMET-H 3.1 and H 3.2, where a considerable fraction of Zr existed in the melt. The measured release rates of the gases generated by the reaction are represented in Fig. 4.3.8. Typical features characterizing the hydrogen curves are the first release during dry concrete erosion and the second release at the onset of flooding. This second release mainly depends on the mass of the metal melt and the energy contained in the melt at the time of flooding. For high metal melts, as used in COMET-H 3.4, it corresponds to about the first release.

The integrated amounts of hydrogen from all experiments are given in Table 4.3.2 above. The increase in the amount of H_2 from 310 g to 1300 g with an increasing mass of the melt is clearly visible.

It is important to relate this amount of H_2 to the molar content of water existing in the concrete, which is potentially available for the chemical reaction. This molar ratio varies between 0.4 for low and 0.7 for high melts according to Table 4.3.2. It can therefore be concluded that the chemical reaction of the steam with the iron is not complete as the residence time of the steam in the melt is not sufficient for a chemical equilibrium to be established. With these figures it is easy to estimate the H_2 release for the reactor case from the amount of concrete water in the sacrificial layer: The integral amount of H_2 varies between 40 and 70% of the molar water content in the concrete.

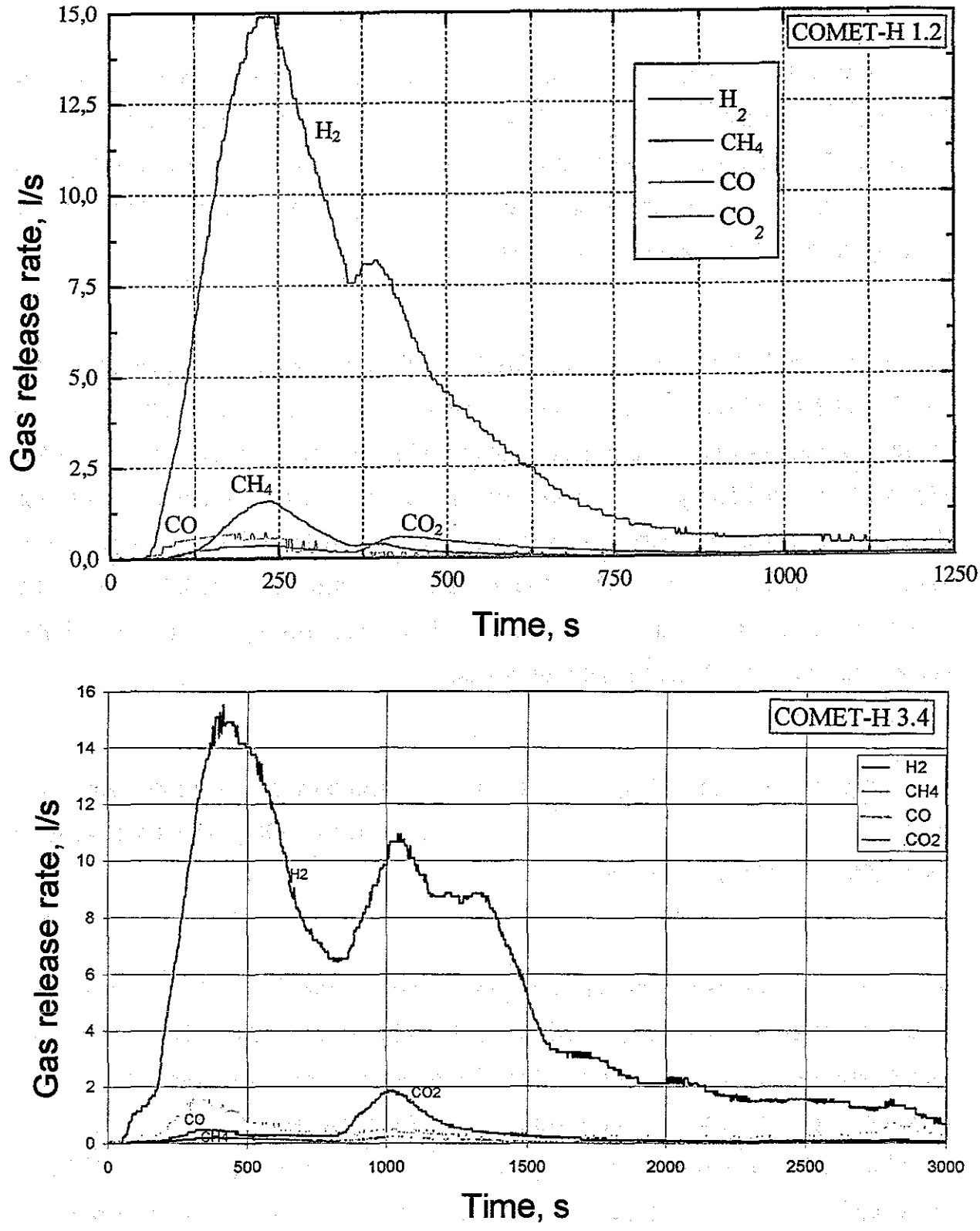

Fig. 4.3.8: **Release rate of gases from chemical reactions in COMET-H 1.2 and COMET-H 3.4**

These ratios are changed considerably when metal zircaloy exists in the melt. Zirconium may also react with other reaction partners, e.g. with the SiO_2 from the concrete, which is then reduced to Si. Si is soluble in the iron melt, and upon the completion of Zr oxidation it is oxidized by continued steam release. The reaction heat released from metal oxidation significantly contributes to the energy balance in the melt. The reactions of Zr and Si with steam are very rapid and therefore take place to the complete extent.

This becomes especially obvious in the experiment COMET-H 3.1, in which the Zr fraction in the melt corresponds to about 60% of the inventory of the fuel cladding. As evident from Fig. 4.3.9, the hydrogen production rate during initial concrete erosion is higher than without Zr by about a factor of 4. This corresponds to a complete conversion of steam at an increased erosion rate. At the same time, SiO_2 is reduced to Si. As the reactions are very rapid, Zr oxidation is completed after about 5 minutes and 70 mm erosion of the sacrificial concrete layer. Hence, the chemical aggressiveness of the melt is strongly reduced. For further formation of H_2, the oxidation of Si is of crucial importance. At the onset of cooling water inflow at 430 s, hydrogen production is increased and accumulates to about one third of the total hydrogen mass.

According to Table 4.3.2, the integral amount of hydrogen released in the COMET-H 3.1 experiment is 2400 g and, hence, much higher than without Zr. This is also reflected by the molar ratio of H_2 to concrete water, which amounts to 1.25. Consequently, more hydrogen is released than produced by concrete erosion alone. This additional hydrogen originates from the contact of the cooling water with the hot melt. As expected, experiment COMET-H 3.2 with only half the content of Zr exhibits a smaller hydrogen release, corresponding to 70% of the concrete water.

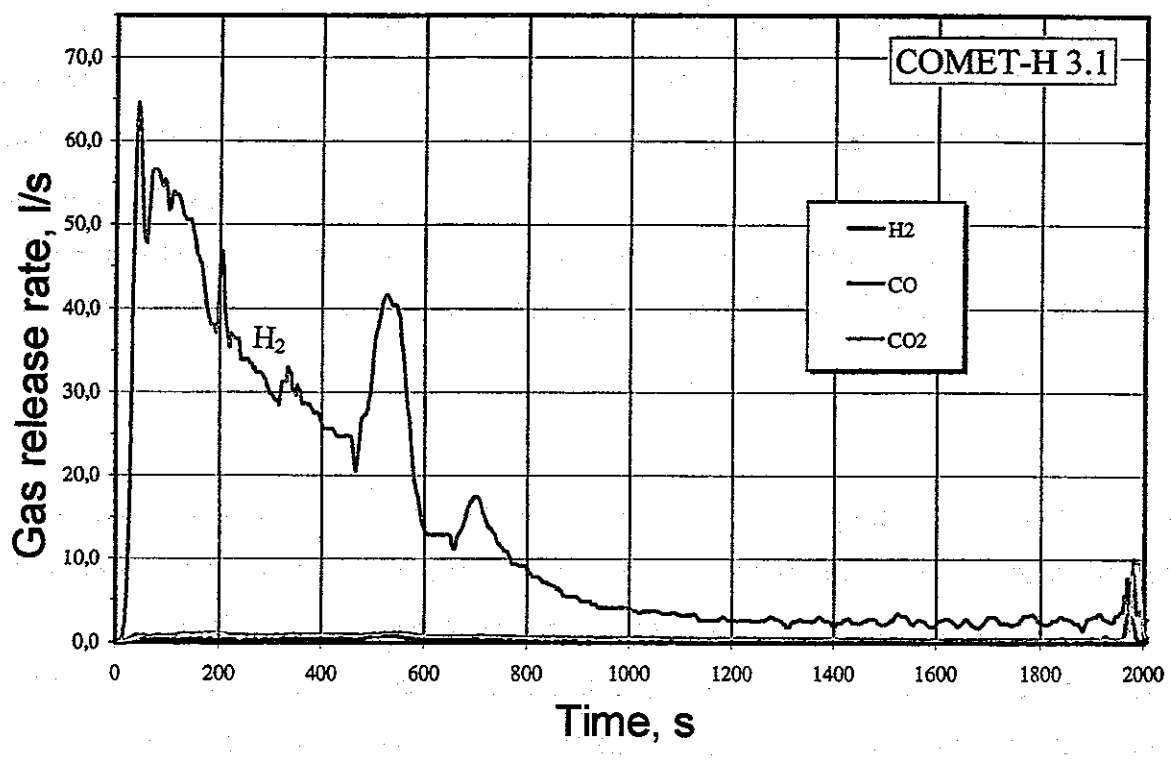

Fig. 4.3.9: **Release rate of gases in the presence of Zr, COMET-H 3.1 experiment**

Aerosol Release

On the one hand, non-radioactive constituents of the concrete and the melt may contribute to aerosol formation during concrete erosion and cooling. On the other hand and from the radiological point of view, the aerosols of the fission products are very important when released from the melt under certain conditions.

Although aerosol formation in the COMET-H experiments is not entirely representative due to the different chemical composition of the oxide melt, the observations made with regard to the aerosol rate and the composition of the aerosols are important for the evaluation of the cooling concept. It is confirmed by the COMET-H experiments that in the melts studied aerosols are generated exclusively by the evaporation and condensation of volatile melt constituents (condensation aerosols). Particles produced by the spraying of the melt as a result of the gas passage are so large that they settle very rapidly and, hence, do not contribute to the aerosols.

The aerosol density in the exhaust gas as a function of time was measured in the experiments by the extinction of a laser beam. It is shown in Fig. 4.3.10 for the experiments COMET-H 3.1 and 3.4. In these experiments, 500 and 1000 g of Mo and oxides of Ba, Ce, La and Sr are added to the melt for the simulation of major fission products. In experiment H 3.1 an additional fraction of 85 kg Zry is contained in the metal Fe-Ni melt to simulate the not yet oxidized cladding material. The experiment COMET-H 3.1 is characterized by the highest aerosol release of all experiments. As soon as the melt is poured in (time = 0), the extinction behavior first exhibits the release of aerosols during the phase of dry concrete erosion. This release is considerably higher in the presence of Zr than in the absence of Zr, as Zr may convert some species into more volatile compounds. Furthermore, the temperature of the melt is higher at first due to the energy introduced by Zr oxidation. In all experiments, a very rapid decrease of aerosol production to nearly zero can be observed when flooding starts. The curve of H 3.4 also shows that the first weak cooling water inflow at 720 s leads to a slower decrease in the aerosol rate until the melt is covered by water at 1300 s. The later aerosol peaks at 2500 and 2700 s result from the destruction of the epoxide material, because the melt has not been cooled down in all sections.

Consequently, aerosol release is actually limited to the short phase of dry concrete erosion. Chemical analysis of filter samples which were clearly identified to be condensation aerosols yields sodium (up to 30 wt.%), followed by potassium (up to 14 wt.%) as the major aerosol constituents. Both are contained in the sacrificial concrete and hence, not radioactive. In contrast to this, only a small amount of boron is released from the glass concrete. The remaining constituents of the melt (Ca, Si, Fe) are hardly encountered. Of all simulated fission products in the presence of Zr, only Sr was proved to be a major contributor to the aerosols (maximum 5 wt.%) in the initial phase of erosion. Its release may probably be caused by the initially high temperature of the melt.

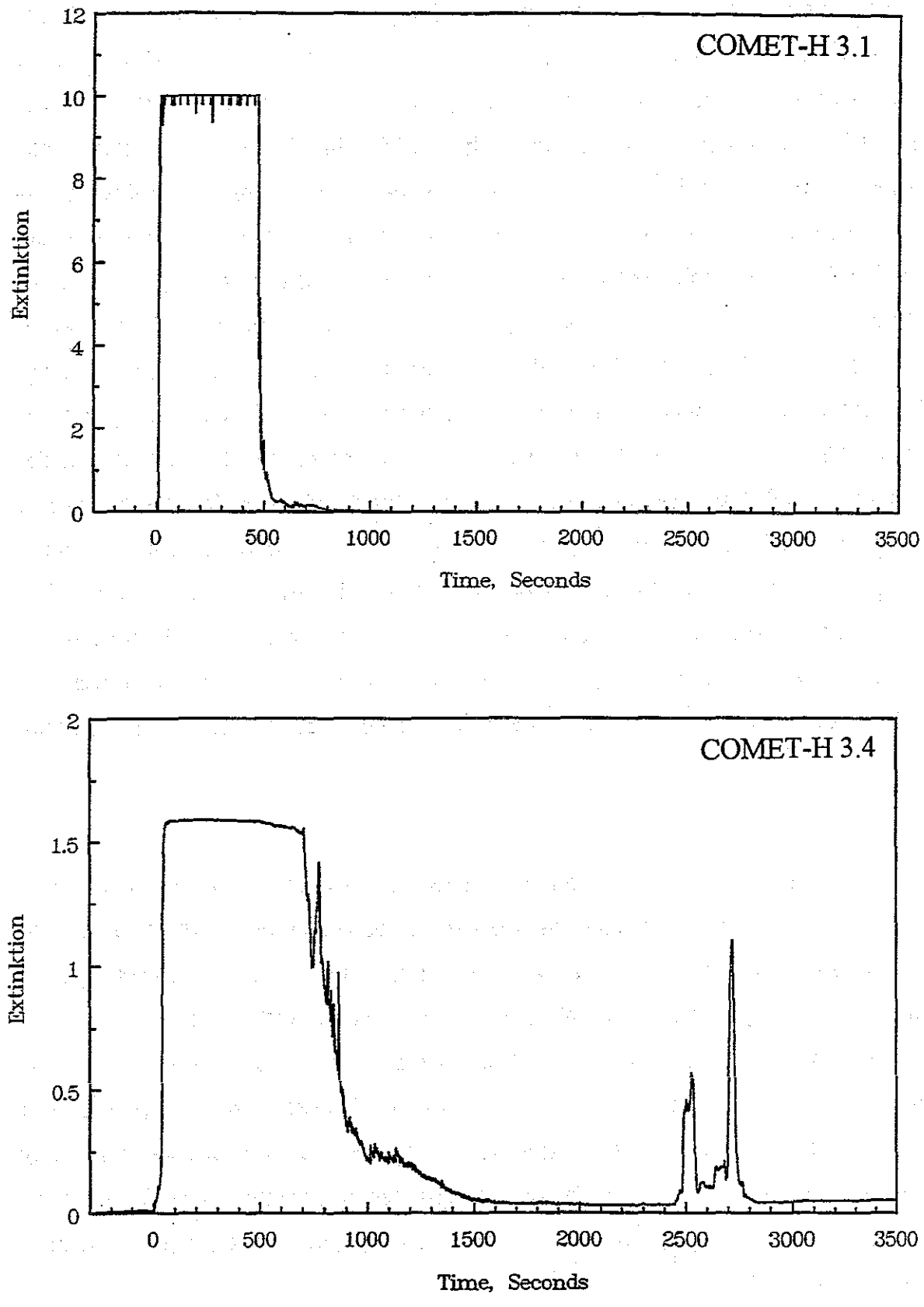

Fig. 4.3.10: **Extinction of a laser beam as a measure of aerosol release in the COMET-H 3.1 and COMET-H 3.4 experiments**

Limits of Coolability

In the COMET-H test series, a variety of conditions was established for the cooling of the melt under continuous decay heat simulation. In all experiments, water penetration from below was found to provide a very effective cooling. Situations of the cooling not resulting in a complete solidification shall be discussed below:

- In COMET-H 2.1 cooling was studied in the case of inhomogeneous erosion. At the same time, the number of melting plugs was halved and the plug distance was increased from 80 mm to 113 mm. In the central area, the coolant water flow through the plugs was rather small. Insufficiently cooled melt of less than 100 g eroded the sacrificial concrete between the plugs down to the epoxide carrier plate. It then penetrated the plate and finally solidified in the water layer.

  The following conclusions can be drawn from this experiment:

  1. The smaller plug distance of 80 mm will be maintained.

  2. The plugs will be embedded into a castable layer of aluminum oxide of higher thermal stability. This layer will reach up to the upper edge of the plugs. This allows the melt to be kept at the level of the plugs until it is fragmented and cooled down sufficiently by the penetrating water.

     This improvement was made in all following experiments and proved successful.

- In the experiments COMET-H 3.2 and H 3.4 the flooding water pressure was reduced from 0.2 to 0.1 bar. At the same time, the melt heights were increased (33 and 50 cm) and in H 3.2 the inlet throttles of the plugs were enlarged. In H 3.2 small amounts of the metal melt (30 –140 g) penetrated through the plugs into the

water layer after a nearly complete solidification had been achieved. Cooling was not endangered.

In H 3.4 which was performed at an increased height of the melt, considerable parts of the melt were fragmented and coolable. In spite of the integrally sufficient water inflow, however, no effective flow channels developed when the plugs opened in the center of the cooling facility, because the driving pressure of the water was too low and the open plugs were blocked by penetrating melt. Thus, a coherent liquid metal section with a surface area of about 400 cm^2 was generated on the ceramic layer. This metal section was heated continuously at a high volume power density, but cooled insufficiently. The weakest points of this arrangement were the plugs embedded into the ceramic layer. After 45 minutes two plugs were penetrated and about 8 kg of metal melt each entered the corresponding two sectors of the water layer. As a result, the plastic cooling facility was damaged considerably. The melt was then cooled down after an automatic shutdown of the decay heat simulation without further components being damaged.

It is obvious from these two experiments performed at a low flooding water pressure that the limits of safe coolability are reached or even exceeded when using very high metals. However, power distribution in the experiments is more critical than in the reactor, as an increased downward heat flux is generated by the release of decay heat only in the metal. Based on the positive results of the remaining experiments and to provide for a sufficient safety margin, an effective flooding water pressure of 0.2 bar should be ensured in the reactor.

4.4 Conclusions with Regard to Normal Cooling, Advantages and Limits

The following conclusions can be drawn from the transient experiments and the experiments with simulated decay heat:

- The **fragmentation of the melt** by water inflow from below is an effective process to attain coolability of the melt. Fragmentation is based on the rapid evaporation of the flooding water that has entered the melt, with a volume expansion by more than a factor of 1000. With the start of solidification, the porous melt structure that is easily passed by the steam/water flow is fixed. Due to their larger solidification range and the increasing viscosity when approaching the solidification temperatures, solidified oxidic melts have a higher porosity than metal melts.

- The **effective flooding water pressure** is a very important parameter for the fragmentation and cooling of the melt. Pressure variation in the range of 0 to 0.4 bar has shown that the cooling rate increases with the pressure, as expected. Even at a differential pressure of 0 bar, a well-cooled and porous melt was obtained in transient experiments. Fragmentation is promoted by the ongoing erosion process of the concrete. Experiments with a simulated long-term decay heat production, however, confirmed that certain parts of the melt may be cooled poorly when the water pressure is low and the melts are very high.

- The **limits of a rapid and complete solidification** of the melt are reached when due to the small water pressure the inflow of flooding water is not sufficient to establish stable flow paths in the melt. Then, the melt may enter the melting plugs from above and block them. Consequently, poorly cooled, liquid parts of the melt remain on the ceramic base layer. Later these parts enter the bottom water layer via the plugs as the weakest points of the arrangement, and in this water they are finally cooled down. Such processes were observed in the heated experiments at 0.1 bar water pressure.

- The experimental conditions in the COMET-H experiments may be less favorable than in a core meltdown accident (the experimental conditions are more demanding because of (i) a higher power density in the metal and (ii) structures made of epoxide instead of steel). Nevertheless, it seems to be reasonable with regard to

the increased EPR melt heights of about 37 cm to select the value of $\Delta p = 0.2$ bar as a **safe design pressure for the flooding water**.

- Taking into account an inhomogeneous erosion of the sacrificial concrete layer, the **duration of the quenching process** is at least 15 minutes until stationary conditions are reached. After this, the melt is completely solidified and its stationary temperature amounts to a few hundred °C only. The cooling rates are accordingly high. At the beginning of flooding, the value is at least 2 MW/m^2 and, hence, considerably exceeds the decay heat power to be removed.

- Safe cooling was demonstrated with **high-temperature melts of different compositions.** The applied simulation melts were based on aluminum thermite with typical initial temperatures of 1900°C and were stratified (metal below oxide) or purely oxidic. Thus, the boundary cases of use under reactor conditions are covered. Additional experiments performed with **prototype UO_2 melts** of 110 and 150 kg also demonstrated the efficiency of cooling for real corium melts.

- Experiments were also performed with an **inhomogeneous erosion** of the sacrificial layer and a resulting local start of flooding and cooling only. Upon the improvement of the concept by the addition of a more stable ceramic base layer reaching up to the level of the melting plugs, the concept now is **sufficiently self-stabilizing**: Cooling is further improved by the opening of additional melting plugs until the melt is cooled down in a stable manner. Surface crusts that form over insufficiently cooled areas due to lateral flooding with the cooling water are broken up with the melt being partly ejected via small volcanoes.

- **Metal zircaloy** possibly existing in the melt is oxidized during the erosion of the sacrificial concrete and the thus generated reaction heat is removed safely. This strongly reduces the high chemical aggressiveness of the melt.

- During cooling **no steam explosions** that may endanger operation occur.

- **Hydrogen release from the melt** ends shortly after the start of cooling. The released molar amount of hydrogen varies between 40 and 70% of the water bound in the sacrificial concrete, depending on the height of the melt. At a very high Zr content, the amount of hydrogen may rise to 125% of this value.

- **Aerosol release** also ends with the start of cooling. The aerosols are mainly generated by concrete constituents.
- Due to the rapid solidification of the melt and its very small temperatures over the long term, the **structures of the cooling facility and their surroundings** remain cold. Like the porous solidified melt, they are wetted by the flooding water. Thus, **long-term coolability** is ensured.
- According to previous experiments, the COMET concept also allows to manage last runnings of secondary melts. This aspect shall be dealt with in Section 5.4.

5. Use of the COMET Cooling Facility in the EPR

5.1 Design of the Cooling Facility

The COMET cooling facility to be used in the EPR may designed as described in Sec. 1, and in Fig. 1.1. The distance of the melting plugs is 80 mm such that 156 plugs per square meter are installed.

The plugs are equipped with burnable caps containing pressed pellets of Mg and $KClO_4$, which were tested in the experiments. The burnable cap was designed and manufactured in cooperation with the Fraunhofer Institute for Chemical Technology (ICT) that has acquired considerable experience in the fields of propellent and explosive materials. In technical applications, potassium perchlorate and magnesium propellents are stable over a long term and non-hygroscopic such that safe long-term operation may be expected. As regards the possible use in the reactor with expected operating times of 60 years, experiments may be performed in a climatic chamber at increased temperatures, if necessary, to simulate aging (private communication R. Ludwig and Dr. Volk, Fraunhofer Institute for Chemical Technology, 1998).

The base plate below the cooling facility is equipped with a liner to ensure the necessary tightness as against the cooling water. To release the air during passive water inflow, the gap below the carrier plate of the plugs is vented via redundant ascending lines into the containment.

As this gap is dry during normal operation and only loaded by water in a core meltdown accident, the cooling facility is not subjected to noticeable aging. If an inspection is required in the gap, it may be performed by means of video or fiber optics via openings that are to be provided in the water supply line.

5.2 Cooling Water Supply

In accordance with the results presented in Sec. 4.4, an effective flooding water pressure of $\Delta p = 0.2$ bar is proposed for safe cooling. This is the value, by which the water pressure at the plug level must exceed the static pressure of the melt upon its spreading at a height of about 37 cm and determines the water level in the flooding tank/IRWST.

As described in Sec. 1, the connection to the flooding tank is established by a valve that opens when the melt enters the spreading compartment. The melting plugs open automatically when the melt has eroded the sacrificial concrete above them.

After the flooding of the melt and the balance of the water levels in the spreading compartment and the IRWST, further water supply at first is only as high as it is needed to compensate for the evaporation losses into the containment. These are about 10 l/s. Assuming that about 20% of the available plugs are passed by the water flow, a water supply rate of 2 cm3 water/s per plug is obtained.

It is envisaged by the EPR conception to accomplish long-term decay heat removal from the containment by an active cooling circuit. For this purpose, water is taken from the IRWST via a pump and a heat exchanger and supplied to the cooling device from below, or introduced into the containment by spraying. To ensure failure-free operation of all components over long terms, water removal from the IRWST has to take place such that coarse, particle-like impurities in the water are retained by a proper position of the discharge lines and adequate filters. Thus, blocking of the cooling channels with a throttle cross-section of 5 mm ∅ is excluded.

However, even an interruption of water inflow from below after the formation of the porous solidified melt would not have any negative impacts on safe cooling. This can be concluded from several COMET-H experiments, in the course of which water

supply from below was interrupted several times during long-term cooling after the complete solidification of the melt. Water supply was interrupted to limit the water level in the test crucible after the solidified melt had been flooded (Figs. 4.3.3a and 4.3.4a). In none of these experiments, major temperatures were found to increase above 100°C. This is due to the high porosity of the solidified melt, which allows for a sufficient inflow of cooling water only from above to all major sections if long-term bottom supply should be obstructed.

5.3 Steam Explosion and Steam Generation during the Cooling of the Melt

Steam Explosions

In all COMET experiments, no major energetic interactions were observed during water inflow from below. The reason mainly consists in the small amount of reactive cooling water that is supplied locally to the melt via the melting plugs. Even in case of a steam explosion, the associated energies are very small. This phenomenon was studied in special COMET-T experiments described in Section 4.1.

When postulating the occurrence of local steam explosions, the maximum loads are encountered on the water side. According to the COMET-T experiments, the water supply has to be designed against local dynamic peak pressures of 10 bar with a pulse width of 5 ms. As far as the static design is concerned, a value of 2 bar over-pressure is on the safe side.

The dynamic pressure peaks of <0.1 bar reached in the gas plenum above the melt are very small.

Loads resulting from steam explosions due to uncontrolled flooding of the melt surface are far more difficult to estimate. In this case, larger amounts of water from the primary circuit may enter the melt via the reactor cavity at a very unfavorable point of time. If such a scenario cannot be excluded, the dynamic loads have to be estimated using methods for the description of steam explosions. Both the carrier structure of the COMET cooling facility as well as the spreading compartment have a very robust design and, hence, a high stability against such loads.

Overpressure in the Spreading Compartment

Evaporation of the water entering the melt leads to a high steam flow which leaves the spreading compartment and enters the containment via an overflow opening of 12 m^2. By means of the following estimation, the maximum overpressure in the spreading compartment as compared to the containment in case of a very high steam flow with a high steam temperature in the initial phase of cooling can be determined.

The following assumptions are made:

Cooling area = spreading area	170 m^2
Specific water inflow	2 kg/s m^2
Total water inflow	340 kg/s
Pressure in the containment	1 bar
Steam temperature	1000 K

Water inflow to the entire cooling area (340 kg/s) is assumed to be very high. By assuming that the inflowing water is evaporated completely, it is neglected that cooling processes on the large cooling surface may be inhomogeneous, as a result of which maximum steam release would be reduced. Therefore, the estimation of a steam rate of 340 kg/s is very conservative. The temperature of the outflowing steam is assumed to be 1000 K. This value corresponds to the short-term maximum temperature measured in COMET-H 3.1, where the energy of the melt was very high due to Zr oxidation.

The overpressure in the spreading compartment as compared to the free volume of the containment is obtained from the pressure loss of steam flow. Here,

$$\Delta p = \varsigma \frac{\rho}{2} u^2$$

applies. Steam density under the above conditions is ρ = 0.22 kg/m^3. This yields a volume flow of the outflowing steam of 1550 m^3/s with a flow velocity u of 129 m/s in the overflow cross-section of 12 m^2. The flow processes are fully turbulent (Re $\approx$ 3 $\cdot$10^7).

The drag coefficient is obtained as the sum of inflow (0.4) and outflow (Carnot diffusor, 1.0), ς = 1.4. This yields the pressure loss of

$$\Delta p = 1.4 \cdot 0.5 \cdot 0.22 \cdot 129^2 \text{ N/m}^2 = 2.6 \cdot 10^3 \text{ N/m}^2 = 0.026 \text{ bar.}$$

This pressure loss corresponds to about 13% of the available flooding water pressure and hardly obstructs the inflow of water into the melt. In reality, much smaller pressure losses are expected. This especially applies to the time after the decline of the first cooling phase, as the steam rate and the steam temperature drop rapidly.

At a constant mass flow of the steam, the variation of the pressure loss with steam temperature and steam pressure can be derived from the above equation as

$$\Delta p \sim \frac{T}{p}.$$

Consequently, the pressure loss decreases further with time, because the steam temperature T drops and the pressure p in the containment increases.

According to the CONTAIN calculations given below, the containment pressure has already risen to 2 bar at the start of cooling. Consequently, the pressure loss is only half of the value estimated above for a containment pressure of 1 bar. As the flooding water tank (IRWST) is open towards the containment, the rising containment pressure does not adversely affect the effective supply pressure of the flooding water.

Pressure Increase in the Containment

As a result of the evaporation of the cooling water, the pressure in the containment first increases with time. This is counteracted by the condensation of the steam at the containment structures and possibly by active cooling.

For calculating the pressure increase in the EPR as a consequence of steam release from the COMET cooling device, the CONTAIN code was applied (W. Scholtyssek, private communication 1998). The calculation was based on the following assumptions:

A rupture of the surge line to the accumulator and failure of all safety systems are assumed to be the initiating event of a core meltdown accident (time 0 s). After 5400 s the bottom of the reactor pressure vessel is penetrated and 300 t of corium are released. After a retention for 1 h in the reactor cavity, during which 70 t of concrete are eroded and mixed into the melt, the melt enters the spreading compartment at 9000 s and spreads completely. The sacrificial layer of the COMET cooling facility is eroded within 15 minutes such that cooling of the melt by water inflow from below becomes effective at 9900 s. It is assumed that the entire energy of the melt ($5.4 \cdot 10^{11}$ J) is removed within 15 minutes (15 minutes quenching time) and converted into steam. As a result, the maximum pressure in the containment is reached after 10800 s. Afterwards, the steam release corresponds to the decay heat production. The volume of the containment is 90,000 m^3. Discretization of the containment in CONTAIN is carried out on the basis of the EPR design.

Figure 5.3.1 shows the calculated pressure behavior in the EPR containment. Hydrogen release into the containment is also taken into consideration. Hydrogen burning and the resulting pressure buildup and energy introduction are assumed when the ignition limit is exceeded. This occurs e.g. after 3000 s when a strong Zr oxidation takes place in the reactor pressure vessel. The maximum pressure calculated for the containment of 6.4 bar is encountered at the end of quenching of the melt. The subsequent pressure drop is determined by the condensation of the steam on the containment structures.

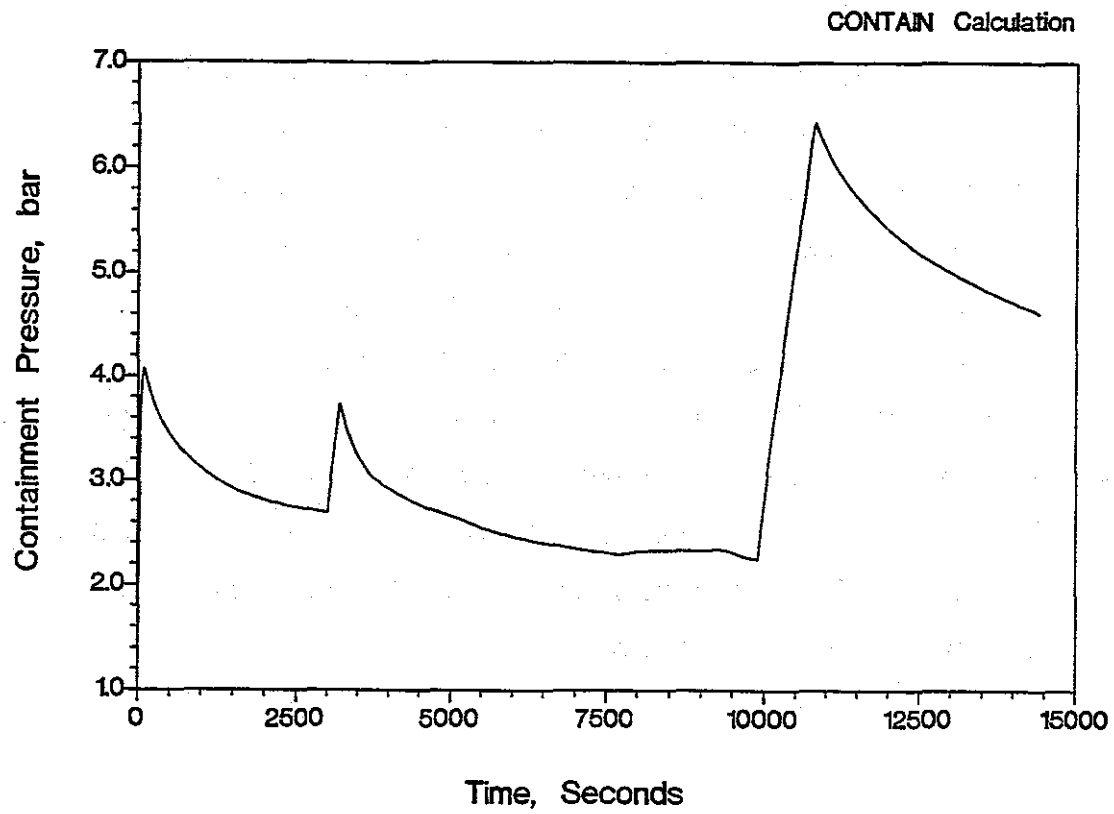

Fig. 5.3.1: **Pressure increase in the EPR containment during a core meltdown accident with complete quenching of the melt by the COMET cooling device within 15 minutes**

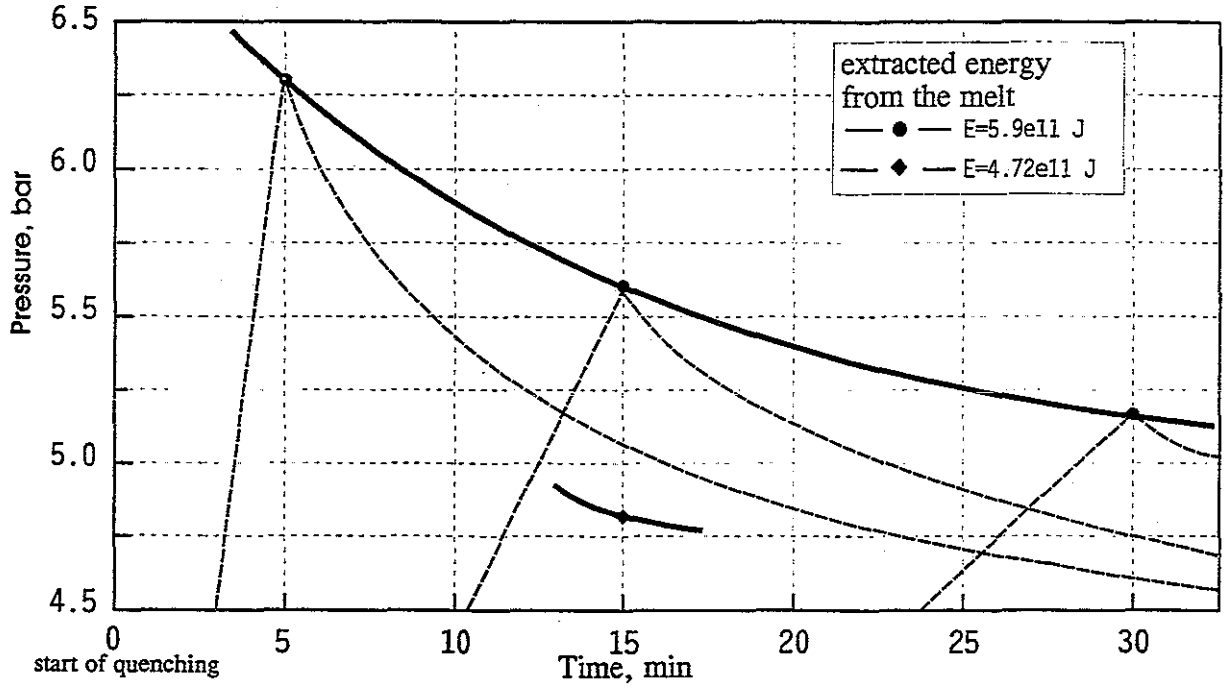

Fig. 5.3.2: **Influence of quench time on the pressure in the EPR during COMET cooling.** —— maximum pressure in the containment as a function of the quench time; ----- pressure history at a quench time of 5, 15 and 30 minutes, respectively

In previous CONTAIN calculations, the influence of the quench time for the melt was studied for a similar accident sequence (W. Baumann, W. Scholtyssek, private communication 1996). The dashed curves in Fig. 5.3.2 show the pressure behavior as of the start of water inflow for quenching times of the melt of 5, 15 and 30 minutes, respectively. As the envelope of these curves, the continuous line shows the peak pressures that are to be expected as a function of the quenching time. A longer quenching time (30 instead of 15 minutes) leads to a maximum pressure that is smaller by about 0.4 bar. Quenching times of less than 15 minutes are not expected due to the large cooling area. In this calculation the pressures are somewhat smaller than in Fig. 5.3.1, because processes taking place prior to the quenching phase also lead to reduced containment loads.

5.4 Changes of the Accident Sequence

Later Runnings of the Melt

As a period of at least 10 minutes lies between the start of melt spreading and the start of cooling by water inflow, there is sufficient time for the spreading of the melt. Even residual melt that flows in from the reactor pressure vessel or reactor cavity during this time is safely bound into the melt.

The question arises, however, whether later runnings of melt can be cooled properly. For this purpose, transient experiments with thermite melts were performed. The experiments focused on later runnings of a melt onto an already solidified melt that is just flooded with water but not yet covered by it. Figure 5.4.1 shows the experimental setup at the time of the secondary melt being poured in.

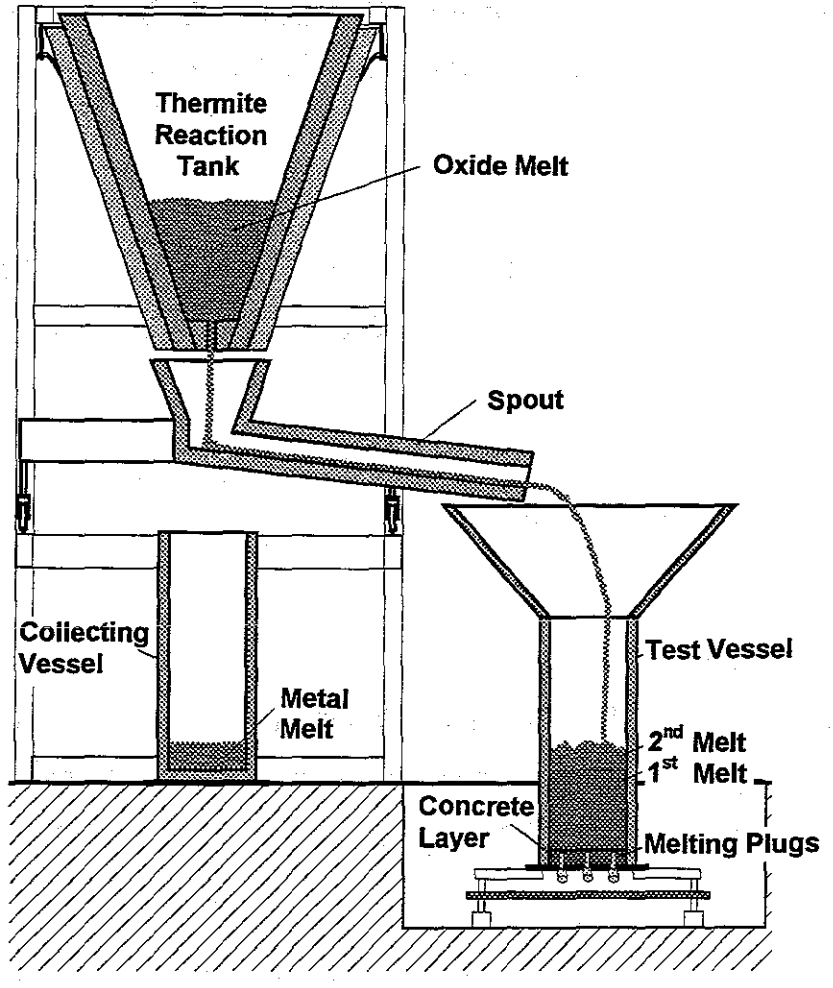

Fig. 5.4.1: **Setup used in the COMET-T experiments for studying later runnings of secondary melts**

Up to now, two experiments have been performed successfully, the results of which are very similar. When the secondary melt is poured in, it gets into contact with the ascending, boiling cooling water. The starting intensive evaporation causes a part of the secondary melt to be granulated and hurled upwards as a melt rain. The major fraction of the secondary melt, which remains in the crucible, solidifies with a very high porosity and can thus be cooled rather well. It is confirmed that the supply of cooling water from below which established during flooding of the primary melt is not reduced by this process such that the safe cooling of the primary melt is maintained, and the flow channels in the primary melt are not blocked by the later runnings of the melt.

It is demonstrated by these experiments that the COMET concept ensures safe cooling of later runnings of secondary melt during flooding of the primary melt. Cooling of the primary melt is not endangered. This is very important as far as safe operation is concerned.

If necessary, the experiments will be continued using a modified geometry of the test setup in order to simulate the lateral inflow of secondary melt after flooding of the primary melt.

Early Flooding of the Melt Surface

With regard to other accident sequences, the question arose as to how the coolability of the melt would be affected by a flooding of the melt surface with plenty of water before the start of water inflow from below. Such a flooding might be caused by an uncontrolled supply of water into the defective reactor pressure vessel.

It must be emphasized that such a massive flooding of the melt in the reactor cavity during melt outflow or on the spreading area is associated with the risk of a steam explosion that than can hardly be evaluated.

As regards the coolability according to the COMET concept, it has to be found out whether the strong cooling of the melt surface may give rise to the formation of such a strong surface crust that a major fragmentation of the melt by subsequent water inflow from below is prevented.

For surface crusts that formed during inhomogeneous erosion of the sacrificial layer with a local onset of flooding from below, it was shown by the COMET-H experiments that these crusts do not prevent a further fragmentation and that sufficient cooling takes place. However, such crusts are probably thin as compared to the crusts which may form upon massive surface flooding and which may be compared with the crusts studied in the MACE experiments. As the MACE experiments show, the investigations of such processes are extremely difficult and the results are strongly limited by the anchoring of the crusts at the periphery of the test facility even in case of a large geometry. In our opinion, the influence of massive surface crusts on the further fragmentation and cooling processes in the COMET concept is not completely clear. According to the experience gained from MACE, it is also impossible to analyze this problem theoretically.

To solve this problem, it seems necessary to exclude the uncontrolled supply of water onto the melt. This would also eliminate the problem of an ex-vessel steam explosion.

6. Modification of the COMET Concept

6.1 Use of Porous Concrete

Based on the positive results regarding the coolability of secondary melts flowing onto the fragmented primary melt, Siemens proposed to replace the field of melting plugs in the COMET concept by a porous, water-filled particle bed. The arrangement is represented schematically in Fig. 6.1.

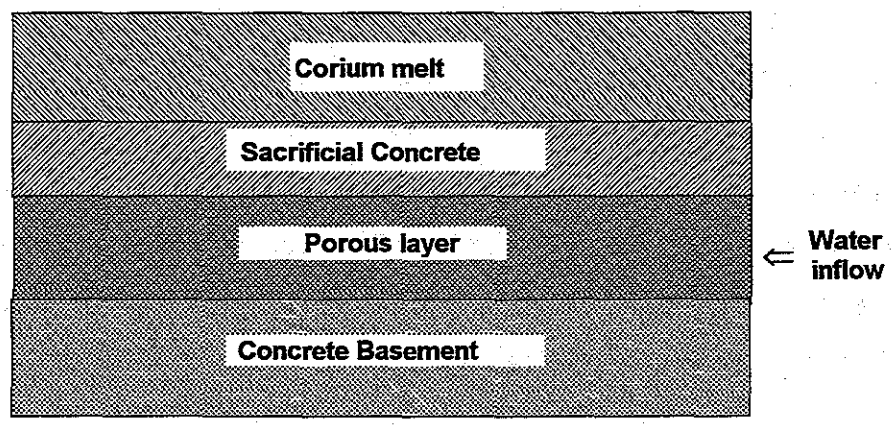

Fig. 6.1: **Modification of the COMET concept by a water-filled porous layer**

According to further conceptions by the FZK and first preliminary experiments, this porous layer shall have the following properties:

- High water permeability in horizontal direction for homogeneous water supply under the entire cooling area
- Limitation of upward water flow to about 1 – 2 l/m^2 s
- Sufficient mechanical stability such that mechanical loads are survived without the porosity being modified

Such a layer may consist of two layers of porous concrete: The bottom layer has a coarse porous structure and, hence, the necessary high permeability for lateral water flow. The concrete layer above with its small porosity and a layer height of about 100 mm serves to limit the upward water flow. The measured compressive strength of such fabricated concrete amounts to about 15 N/mm^2. This corresponds to 50% of the value of ordinary concrete and, hence, is entirely sufficient.

This arrangement has the advantage of an extremely simple setup. Safe operation has to be investigated with the properties of the porous layers being optimized to meet the various requirements. Here, the results obtained in the previous experiments may be used in many respects.

6.2 First Experimental Results

Up to now, three transient experiments have been carried out for the modified COMET concept in the COMET-T test facility of 350 mm inner diameter. Thermite melts of 54 and 180 kg at initial temperatures of 1800°C were used. For the experiments, a porous concrete layer with the desired permeability for water inflow from below was produced.

In all experiments, the erosion of the sacrificial layer was followed by a rapid cooling as soon as the porous concrete layer was reached. Hence, the melt quickly solidified. When using a suitable low-porous concrete, the inflow rate of the cooling water (about 350 cm^3/s) was comparable to that of earlier experiments with the melting plugs. This flooding rate is mainly determined by the porosity of concrete. The effective supply pressure of the flooding water amounted to 0.1 bar in these experiments. Steam explosions or more vigorous melt-water interactions during the inflow of cooling water did not occur.

The porous concrete layer was not attacked by the melt advancing from above. It thus proved to be a safe barrier. Its porosity was fully maintained and not affected by

the possibly penetrating melt. Thermocouples in the upper part of this layer show that due to the water existing in the pores the temperatures in the layer hardly increase even in the contact zone of the hot melt.

The porosity of the solidified melt is sufficiently high in the upper oxide layer and comparable to that of earlier experiments. It remains to be verified in future experiments, whether flow through the bottom metal layer is sufficiently homogeneous to exclude uncooled regions.

6.3 Outlook

The modified COMET concept using a porous, water-conducting concrete layer represents an interesting variant that should be further investigated with regard to its use in the EPR. For this purpose, additional transient experiments will be useful. They should be supplemented by experiments with sustained heated melts in the COMET-H test facility.

Advantages of this variant include the very simple and low-cost setup as well as the high stability of the water-conducting concrete layer against the melt. Thus, melting of this layer is not expected even in case of small coolant water pressures.

Possible drawbacks may consist in the fact that due to the non-localized inflow of the flooding water into the melt, which took place via the plugs up to now, water access to the area may be less homogeneous and, hence, fragmentation of the melt may also be less homogeneous. However, partial areas of the melt that may be cooled insufficiently would be stabilized by the water-conducting layer. As the inflowing amounts of water may possibly be distributed less homogeneous, the interaction between the melt and the cooling water may be more vigorous. The experiments performed up to now, however, do not give any indications that might endanger this variant.

7. Summary and Conclusions

The COMET concept for cooling core melts is described with regard to its applicability in the EPR. According to the concept, the melt is passed onto a horizontal area, where a layer of sacrificial concrete is eroded first. In this phase of dry concrete erosion, the melt can spread completely and part of its energy is absorbed by concrete decomposition. Following the erosion of the sacrificial layer, the channels located in the bottom layer are opened by the hot melt and passive inflow of the cooling water from below takes place, driven by the pressure of an elevated water storage tank (IRWST). The rapidly evaporating water breaks up and fragments the melt, and passes it in the form of a water/steam mixture. This leads to the generation of large internal surfaces, via which the decay heat can be removed safely from the melts for both the short and the long term. The high heat removal allows the melt to solidify completely as a porous bed after a short time. This bed is filled with water and flooded. Thus, the state of safe long-term cooling is achieved.

In various experiments, the major processes during fragmentation and cooling of the melt were investigated. Very detailed experiments were performed with high-temperature thermite melts, in the form of transient tests or with decay heat simulation. These experiments were supplemented and confirmed by another two experiments using UO_2-containing prototype corium melts.

The cooling initiated by bottom flooding is characterized by a rapid and complete solidification of the melt that is supposed to occur in the EPR within a period of 30 to 60 minutes. Hence, the attack of the melt is limited to a clearly defined time and local range of the sacrificial concrete. The temperatures of the carrier structures of the cooling facility and their surroundings remain cold such that no special material loads occur in this area.

This rapid heat removal from the melt results in a high release of steam. The resulting short-term maximum pressure in the containment was determined for a core

meltdown accident under the assumption of the entire energy of the melt being extracted within 15 minutes only. It amounts to about 6.5 bar. This pressure is rapidly decreased by the condensation of the steam on the cold structures of the containment. In spite of the high steam flow, pressure differences between the spreading compartment and the containment are so small that they do not interfere with the cooling process.

It was demonstrated that steam explosions and the presence of zirconium metal in the melt do not cause any problems with regard to the cooling concept. Hydrogen and aerosol releases end shortly after the start of cooling. The released amounts of hydrogen correspond to about 40 to 70% of the molar water content in the sacrificial concrete.

For the safe operation of the cooling facility, an effective water pressure of 0.2 bar or higher is proposed in accordance with the experiments performed. Under the conditions of continuous decay heat simulation at smaller water pressures (0.1 bar), it was found out that partial areas of high melts may be cooled insufficiently. The melt may then penetrate through the melting plugs into the bottom water layer.

It was also shown at an effective water pressure of 0.2 bar that locally inhomogeneous or increased erosions of the sacrificial layer and the resulting start of local cooling only are compensated by the improved stability of the ceramic base layer. Surface crusts that develop under these conditions are broken up until the necessary fragmentation and cooling of the melt are achieved.

In addition, the later inflow of a melt onto an already solidified primary melt during flooding was investigated in the experiments. Cooling of the primary melt is completely maintained and the secondary melt solidifies in a fragmented form that can be cooled easily. If necessary, these experiments may be extended to cover conditions, where the primary melt has already been flooded by water.

The consequences of an early massive water inflow onto the surface of the melt prior to the water inflow from below are, however, not clear. With regard to further problems that may result from possible steam explosions in such a scenario, it seems to be necessary to exclude such an uncontrolled water inflow from above.

Based on these results, a reliable design and operation of the COMET cooling facility in the EPR seems to be possible.

In a **concept variant** a porous, water-conducting concrete layer is used instead of a field of melting plugs. First experiments show that a good cooling of the melt and a high resistance against downward erosion can be expected. Further experiments should be performed to study the potential of this very simple and cheap solution.

8. References

[1] Alsmeyer, H., Tromm, W., "A Core Catcher Concept And Basic Experimental Results", Int. Topical Meeting on Safety of Thermal Reactors, July 21-25,1991, Portland, OR

[2] Tromm, W., Alsmeyer, H., Schneider, H., "Fragmentation of Melts by Water Inlet from Below", Proc. 6th Int. Topical Meeting on Nucl. Reactor Thermal Hydraulics (Nureth 6), Oct. 1993, Grenoble, France, 99 - 106

[3] Tromm, W., Alsmeyer, H., "Experiments for a Core Catcher Concept Based on Water Addition from Below", Nuclear Engineering and Design 157 (1995) 437 - 445

[4] Tromm, W., "Experimentelle Untersuchungen zum Nachweis der langfristigen Kühlbarkeit von Kernschmelzen", Wissenschaftliche Berichte, FZKA-6176 (Nov. 1998), Thesis, University Karlsruhe 1998

[5] W. Tromm, H. Alsmeyer, M. Bürger, W. Widmann, M. Buck, "COMET Experiments and Theoretical Modelling", FISA-95 Symposium - EU Research on Severe Accidents, Luxembourg, Nov. 20-22, 1995

[6] Alsmeyer, H. et al., Molten Corium Concrete Interaction Project, Final Progress Report, Luxembourg, EUR 17126 EN (1995), 315 - 379

[7] Tromm, W., Alsmeyer, H., et al., "Experiments and Theoretical Modelling for a Core Catcher Concept for Future Light Water Reactors", 31st Nat. Heat Transfer Conf., Houston, AICHE Symposium Series, Vol. 92 , 310 (1996), 304 – 309

[8] Alsmeyer, H., Farmer, M., Ferderer, F., Spencer, B., Tromm, W.; "The COMET Concept for Cooling of Ex-Vessel Corium Melts", 6th International Conference on Nuclear Engineering ICONE-6, San Diego, Calif., May 10-15, 1998, New York, N. Y.: ASME, 1998, CD-ROM